

Florida State University Libraries

2015

Miocene Arc Magmatism in Bocas Del Toro, Panama, and It's Constraints on Mantle Wedge and Tectonic Change

Ruiguang Pan



FLORIDA STATE UNIVERSITY
COLLEGE OF ARTS AND SCIENCES

MIOCENE ARC MAGMATISM IN BOCAS DEL TORO, PANAMA, AND IT'S
CONSTRAINTS ON MANTLE WEDGE AND TECTONIC CHANGE

By
RUIGUANG PAN

A Thesis submitted to the
Department of Earth, Ocean, and Atmospheric Science
in partial fulfillment of the
requirements for the degree of
Master of Science

2015

Ruiguang Pan defended this thesis on Nov. 10, 2015.

The members of the supervisory committee were:

David Farris
Professor Directing Thesis

Stephen Kish
Committee Member

Leroy Odom
Committee Member

William Parker
Committee Member

The Graduate School has verified and approved the above-named committee members, and certifies that the thesis has been approved in accordance with university requirements.

ACKNOWLEDGMENTS

I'm very happy to present my thanks to the Department of Geology at Florida State University, and fell really lucky to choose Dr. David W. Farris' research group to continue my studies on geochemistry and tectonics. During my graduate in-depth research program, I learned how to develop a project, specifically including how to read papers, how to analyze data and how to solve specific geologic problems. First, I want to give my deep appreciation to my supervisor, Dr. David Farris, for his full support and kind instructions on my research, especially in my project conducting and paper writing.

Also, my thanks go to my colleagues in our research group, Gary Fowler, Kelci Mynhier, Evan Yokum, Abdulaziz Samkari, Ali Can Altintas. Due to our weekly meeting, we learned a lot from each other through presenting our own research progress and all-around discussions.

Moreover, I would like to give my thanks to my committee members, Professor Stephen Kish, Professor Leroy Odom and Professor William Parker, for their advice on my study and research. My grateful thanks go to Dr. Kish for his kindness on instructing my research and supervising my study and research progress, and beyond.

In the end, my thanks go to all the Department faculty and graduate students. Thanks for their support and help during all my time at Florida State University.

TABLE OF CONTENTS

List of Tables	vi
List of Figures	vii
Abstract	ix
1. INTRODUCTION	1
1.1 Project Description.....	1
1.2 Research Background	1
1.3 Research Significance	3
2. GEOLOGIC SETTINGS	4
2.1 Formation of Panamanian Isthmus	4
2.2 Stratigraphy and Volcanic Lavas in the Bocas del Toro Basin	7
2.3 Ages of the Volcanic Lavas in Bocas del Toro.....	7
2.4 Lithology and Mineralogy	7
3. ANALYTICAL METHOD AND DATA COLLECTION.....	10
3.1 Sampling and Data Collection	10
3.1.1 Sampling	10
3.1.2 Data Collection	10
3.1.3 Experimental Methods.....	11
4. GEOCHEMISTRY	12
4.1 Major Element Chemistry.....	12
4.2 Trace Element Chemistry	16
4.3 Isotope Geochemistry	18
4.3.1 Pb-Nd isotopes.....	18
5. GEOCHEMICAL MODELS	22

5.1 Fractional Crystallization Model	22
5.1.1 Parameters of the Modeling	22
5.1.2 Outcome of the Modeling	24
5.2 Isotopic and Trace Element Partial Melting Model	25
5.2.1 Isotopic Element Model	25
5.2.2 Trace Element Model 1	25
5.2.3 Trace Element Model 2	27
5.2.4 Arc Basalt Simulating	28
6. DISCUSSIONS	31
6.1 Previous Geochemical Models and Evaluation	31
6.2 Arc-hotspot Interaction and Magma Origin	35
6.3 Low-Pressure Fractional Crystallization and Extensional Tectonics	35
7. CONCLUSIONS	37
APPENDIX A: TABLES	39
References	45
Biographical Sketch	49

LIST OF TABLES

A. 1 Major and trace element compositions of Bocas del Toro.....	39
A. 2 Mineral-melt distribution coefficients and bulk distribution coefficient	41
A. 3 Modeled #1, #3 Components and melts for the southern Central American lavas (Gazel et al., 2009)	42
A. 4 Compositions of Model #2, #3 components (Eiler et al, 2004)	43
A. 5 Outcome of modeling of basalts in the Bocas del Toro Basin (Eiler et al., 2005).....	44

LIST OF FIGURES

2.1 A-C. Reconstruction of the Panamanian Isthmus at different geological times (Coates et al., 2013); D. Fracturing of the Panamanian Isthmus during the collision caused two extensional zones, Bocas del Toro and Canal Basin (Farris et al., 2011).	4
2.2 Paleogeographic reconstruction of the Panama arc block and northwestern South America during middle Miocene times	5
2.3 Simplified geologic map of the Bocas del Toro Basin, showing the sampling locations and the distribution of Punta Alegre and Valiente Formations in the Valiente Peninsula (Coates et al., 2003, 2005).	6
2.4 Field interbedded lava flows and sedimentary rocks formed in the coastal environment.	8
2.5 Microscopic pictures of the Bocas del Toro samples	9
3.1 Map of sample locations (six groups are illustrated in different icons and colors).	10
4.1 Major element chemistry of the Bocas del Toro rocks.	13
4.2 Chemical classification and nomenclature of volcanic rocks displayed in total alkali vs. silica (TAS) diagram according to Le Maitre et al. (1989) and Le Bas et al. (1991).	14
4.3 Subdivision of subalkaline rocks after Rickwood (1989) based on the basis of K_2O vs. SiO_2	14
4.4 a. AFM diagram for the tholeiite and calc-alkaline evolution series (Thompson, 1976); b. FeO^*/MgO vs. SiO_2 diagram shows that the rocks can generally be divided by the tholeiite and calc-alkaline boundary.	15
4.5 Trace element patterns of the different group components.	16
4.6 Hf/3-Th-Ta diagram (Wood, 1980).	17
4.7 A. (Ba/La) _N vs. (Ta/Sm) _N diagram; B. Th/Yb vs. Ta/Yb diagram; C. Plot of Ba/Yb vs. TA/Yb for magmatic rocks; D. La/Yb vs. Ta/Yb diagram	18
4.8 Pb and Nd isotopic ratios for samples of the Oligocene-Pliocene samples, the central Costa Rican and Nicaraguan volcanic front lavas, and alkaline basalts and adakites from Costa Rica and Panama	19
4.9 Sr-Nd-Pb isotope diagrams. A. $^{87}Sr/^{86}Sr$ vs. tholeiite, calc-alkaline, backarc alkaline, adakite and Cocos island diagram; B. $^{143}Nd/^{144}Nd$ vs. $^{87}Sr/^{86}Sr$ diagram; C. $^{87}Sr/^{86}Sr$ vs. $^{206}Pb/^{204}Pb$ diagram.	20

5.1 GUA 33 MELTS major element modeling of different groups of volcanic rocks with 0.1, 0.5, 1.0, and 5.0 kbars in pressure.....	23
5.2 Mass and mineral crystallization curves for GUA 33, GUA 27, PAN-06-039 and PAN-06-052 in 1kbars pressure.	24
5.3 Mixing lines connecting the modeled mean Seamount Province melt ($^{143}\text{Nd}/^{144}\text{Nd}=0.51286$, $^{206}\text{Pb}/^{204}\text{Pb}=19.390$, $^{208}\text{Pb}/^{204}\text{Pb}=39.284$) and the mean Cocos/Coiba Ridge melt ($^{143}\text{Nd}/^{144}\text{Nd}=0.51297$, $^{206}\text{Pb}/^{204}\text{Pb}=19.296$, $^{208}\text{Pb}/^{204}\text{Pb}=38.930$) (Hoernle et al., 2000; Werner et al., 2003) with the DM (inverted from sample SO144-1) from Werner et al. (2003).....	26
5.4 A: Model #1, and B: Model #2 for partial melting processes.....	28
5.5 Best fit model solutions shown compared to exemplar basalts.	30
6.1 Age distribution of arc rocks in central and western Panama and in southern Costa Rica (Wegner et al., 2010)..	32
6.2 Abratis et al.' schematic model of subduction zone beneath Costa Rica showing disruption of Cocos plate as result of the collision and subduction of extinct spreading ridge (Cocos Ridge).....	33
6.3 Farris et al.' model regarding the Panamanian tectonic evolution and its effect on the geochemical element changes.....	34

ABSTRACT

The Panamanian Isthmus presents an ideal opportunity to study arc magmatism, arc-hotspot interaction, and the effects of the South America-Panama collision. These effects include changing mantle wedge compositions and localized tectonic activities in western Panama. The Bocas del Toro sedimentary basin contains interbedded Miocene volcanic lava flows that range in age from 12 Ma to 8 Ma and sit behind the main body of the arc.

The volcanic rocks of Bocas del Toro consist of trachy-basalt to trachy-andesite with SiO_2 content ranging from 45 wt. % to 64 wt. %. The MgO content is relatively low ranging from 0.35 wt. % to 3.43 wt. %, and with moderate depletion in FeO (3.9 wt. %-8.0 wt. %) and CaO (2.8 wt. %-10 wt. %). However, K_2O content is extremely high (2.0 wt. %-5.2 wt. %), and these rocks are among the most alkaline in Panama. In terms of trace element geochemistry, the Bocas del Toro rocks exhibit a distinct, but decreased slab dehydration signature with a low Nb-Ta anomaly, enriched fluid-mobile LILEs and low Ti content. We have grouped Miocene and younger western Panama and eastern Costa Rica volcanic rocks into five groups: main arc tholeiite (~17-11 Ma) and calc-alkaline (~12-8 Ma), Bocas del Toro (~12-8 Ma), backarc alkaline (~8-2 Ma), and adakite (<2 Ma) groups. In terms of trace element ratios, the Bocas del Toro rocks have relative low Ba/La, and have values that are higher, but approach the Cocos Ridge, that tracks of the Galapagos hot spot. The La/Yb and Th/Yb vs. Ta/Yb also show values that plot between the tholeiite and general calc-alkaline groups. Overall, trace element geochemistry indicates that an enriched OIB-like component mixed into the melts of the mantle wedge.

With constraints from referenced Pb-Nd-Sr isotopes and the pattern of trace element geochemistry, the data range of the Bocas del Toro samples should be distributed close to the general calc-alkaline and backarc alkaline groups. According to the trace element geochemistry and isotope modeling, the percentage of enriched (OIB / Cocos track) geochemical component mixed into the melts of the mantle wedge, was quantified at 1-3%. Moreover, the pattern indicates that, as arc evolution continued, a progressively greater enriched geochemical components mixed into the wedge melts.

Geochemical modeling allows estimates of the pressure, temperature etc., conditions under which magma formed. The MELTS software was used for major element modeling and show that the Bocas del Toro rocks underwent low-pressure (0.5-1.0 kbars) fractional crystallization, from

1200 ° C to 900° C with 50%-55% fractionation from a starting magma with ~11 wt. % MgO. In addition, trace element models and the ARC BASALT SIMULATOR 3.0 were used to simulate partial melting in the mantle wedge. These models indicate a component of enriched OIB-like mantle. The simulator also shows that the mantle wedge underwent 3.5%-6.0% of melting fraction under dry conditions at pressures of 1.8 Gpa to 1.9 Gpa (~60km) with temperatures of 1150-1350°C. In conclusion, we suggest that the geochemical variations of Bocas del Toro were caused by an influx of an OIB-like component into the mantle wedge by 12 Ma, and that possible effects from crustal extension reduced the overall subduction signature.

CHAPTER 1

INTRODUCTION

1.1 Project Description

This project is a continuation of previous research concerning the arc magmatism, geochemistry and tectonics associated with subduction activities in Bocas del Toro, Panama, conducted by Farris et al. (2011). The previous studies focused on the geochemical anomalies for the fluid mobile large-ion lithophile elements (LILEs) (e.g., Cs, Rb, Ba), and the geologic causes from geologic and tectonic changes, especially regarding extensional magmatism and basin formation. However, petrogenesis processes regarding the partial melting of the mantle wedge and fractional crystallization for the primary magma still need to be quantitatively studied to support the proposed localized arc magmatism model. Therefore, a new geochemical dataset were presented, and an upgraded model for the Bocas del Toro arc magmatism was constructed to determine linkages with the localized crustal extension. In addition, it helps evaluate the influence of tectonics on the magmatic evolution of the Panamanian subduction zone and explain variations in the geochemical composition of presented arc rocks. Multiple approaches including measurement of major/trace elements, isotopes, petrology and modeling of chemical processes were integrated to examine the partial melting process, mixing of different material sources and possible hidden large-scale structures. In summary, these following geochemical and tectonic studies on Bocas del Toro volcanic rocks provide more evidence regarding the hypotheses about the magmatic process, tectonic change, and the formation of the Panama Isthmus.

1.2 Research Background

Subduction zones are geologic sites of the Earth's associated with explosive magmatism and associated geologic hazards. They are also important geologic sites of mass exchange between the continental crust and the mantle, and are thus the fundamental agents in the evolution of the crust-mantle system and tectonic collision. In Panama, the main foci of geologic research are: (1) Dating and processes of closure of the Panama Isthmus (Coates et al., 1992; Coates et al., 2005; Barat et al., 2014; Montes et al., 2015); (2) Geochemical evolution of igneous rock and magmatic history during the formation and closure of the Central American land bridge in Panama arc block

(Wegner et al., 2007, 2010); (3) The enriched chemical signature and tectonic effects of the Galapagos hotspot and the hotspot tracks it generated on the Panamanian arc block, petrologic evolution, and continental genesis in subduction zone system (Hoernle et al., 2000, 2002, 2004; Werner et al., 2003; Gazel et al., 2009, 2011, 2015); (4) Local and regional geochemical variations in Central American arc lavas are controlled by the compositions of subducted sediment inputs (Patino et al., 2000); (5) The petrogenesis of the voluminous Quaternary adakitic magmas and crystal fractionation processes at Baru volcano (Hidalgo and Rooney, 2010, 2014; Hidalgo and Vogel, 2011; Hidalgo, 2012). All of the previous work provides us a fundamental background and base for studying the genesis and evolution of the Panamanian arc isthmus and the arc magmatism in this area.

The previous research in Panamanian Isthmus has focused on when and how the collision between South America and the Panama block initiated in a general sense, and the influx of enriched geochemical component in Costa Rica. However, magmatic variations and effects of tectonic evolution in specific areas in Panama are relatively unexplored areas of research. Farris et al. (2011) initially examined the Bocas del Toro area as an extensional basin due to the transformation of local tectonic dynamics. There, Farris et al. measured the geochemical data and found certain chemical anomalies with respect to other Miocene arc volcanic rocks in Panama. Based on this geochemical data, Farris et al. (2011) found that the volcanic rocks are less hydrous in the canal area than other regular subduction products. The uncommon phenomenon may be caused by the influx of Pacific asthenosphere into the Caribbean realm through the slab-window underneath backarc zone, which was formed via spreading ridge subduction (Abratis and Worner, 2001). By using geochemical and isotopic evidence of volcanic rocks from the Cordillera de Talamanca area, Abratis and Worner (2001) found that some young samples from the Limon Basin, which bear a strong volcanic backarc signature, are signified by high value of Nb/Zr ratio, however, a lower value in Ba/La ratio, relative to other volcanic rocks. These chemical characteristics match geologic process of asthenospheric upwelling through a slab window, coupled with decompression of this Pacific mantle induced by partial melting and hotspot magmatism. An alternative explanation for the enriched mantle component is trench-parallel mantle flow which brought the enriched component from relatively depleted mantle with a long history of interaction with the subducting Cocos plate (Herrstrom et al., 1995) to the current geologic sites. The OIB-signature hosted in the Bocas del Toro arc rocks can also be caused by mixing of ~ 0.5% Galapagos hot spot

from the subducted slab, which is composed of a major part of Galapagos tracks (Gazel et al., 2009). These plume-like materials can also come from the OIB-signature mantle wedge (Eiler et al., 2000, 2005). By mixing different percentages of the end-member source materials (mantle wedge, uppermost sediments and interior altered oceanic crust (AOC) in the subducted slab) together, Gazel et al., (2009, 2011) proposed that the trace element and isotopic modeling of the arc-hot spot interaction in southern central America quantified the contributions from the Galapagos hot spot (Cocos Ridge and Cocos Seamount Province) along the volcanic front from central Costa Rica to NW Nicaragua. Eiler et al., (2000, 2005) reported that the chemical compositions of a low- $\delta^{18}\text{O}$, water-rich component (slab interior) and a high- $\delta^{18}\text{O}$, water-poor component (slab sediments) extracted from the subducting Cocos slab and the flux melting in the overlying mantle wedge by studying the oxygen isotope constraints on the sources of Central American arc lavas. Based on these studies, Eiler et al. explained observed chemical variations in Central American arc lavas by modeling partial melting process. Patino et al. (2000) also suggested that local and regional variations in Central American arc lavas are controlled by variations of subducted sediment inputs through studying core samples from DSDP Site 495. These chemical variations, enriched in LILE elements and with moderate high Ta relative to other samples in Bocas del Toro arc rocks are interpreted as the products of low degrees of decompression melting in compositionally similar asthenosphere and the flux of a plume-like enriched mantle component, possibly related to localized extensional arc magmatism occurred during the Miocene period (Coates et al., 2003; Farris et al., 2011).

1.3 Research Significance

This study will have important implications regarding the types of variations of the magma reservoirs during subduction and collision processes, the causes of temporal-compositional variations in eruptive products within the Panama Isthmus. It also will provide insights into the nature and heterogeneities of the slab-derived or tectonic-transformation-caused melts over a small spatial scale within the Panamanian block. Moreover, it will help understand the arc-hot spot interaction and generation of continental crust in oceanic arcs. All of these potential outcomes have broader impacts on the research of global tectonic and magmatic activities within subduction zones.

CHAPTER 2

GEOLOGIC SETTINGS

2.1 Formation of Panamanian Isthmus

There are competing views as to the age and processes for the continental collision between the Panama arc block and South American Plate, and the resulting closure of Central American Seaway. Coates et al. (2013) present a geological model for the tectonic collision between the Panama arc block and South America plate based on the geology of the Darien sedimentary basin in the Darien region in eastern Panama (Fig. 2.1 A-C). Coates et al. (2013) suggested that collision begins at 12-13 Ma and then complete isthmus formation final closure occurs in the Pliocene (4-

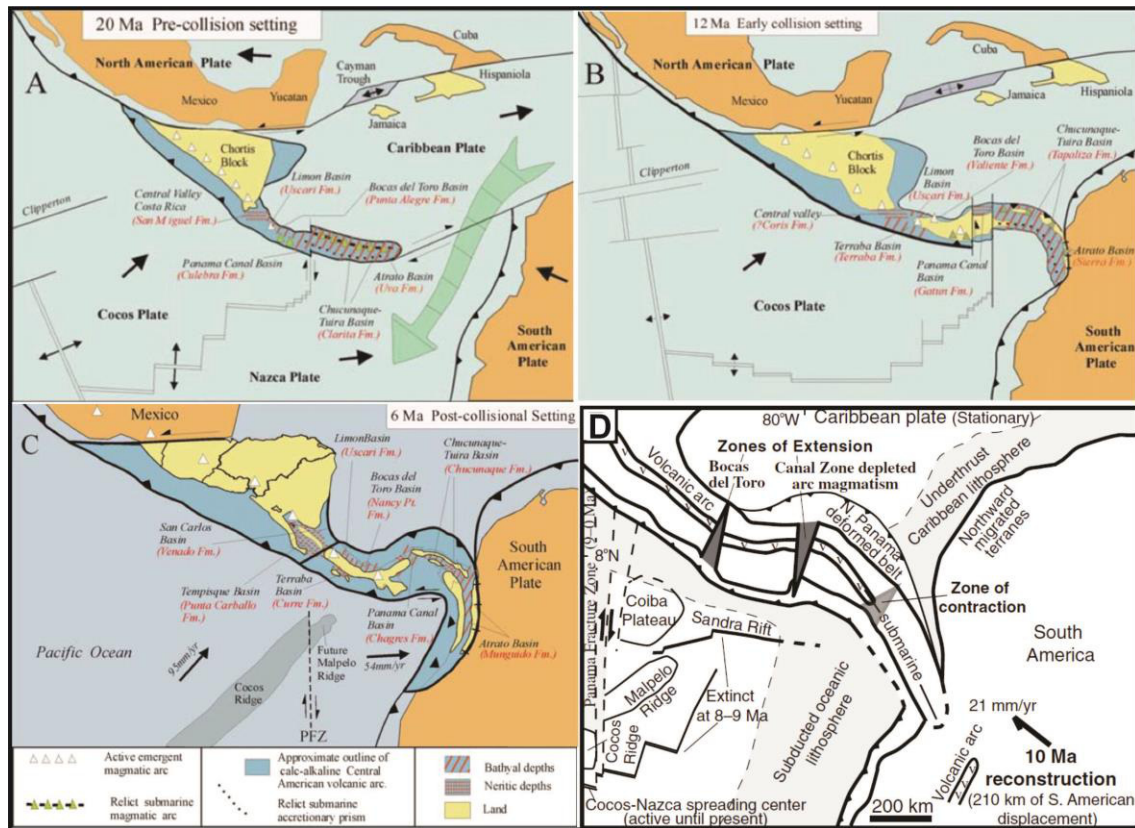


Figure 2.1 A-C. Reconstruction of the Panamanian Isthmus at different geological times (Coates et al., 2013); D. Fracturing of the Panamanian Isthmus during the collision caused two extensional zones, Bocas del Toro and Canal Basin (Farris et al., 2011).

3 Ma). The evidence for the collision is based on geological mapping, biostratigraphy and paleobathymetric analysis of the sediments ranging from upper Cretaceous to upper Miocene. This collision event started the rise of the Panama land bridge and led to the formation of Panama Isthmus.

Farris et al. (2011) identified a transformation from hydrous mantle-wedge-derived arc magmatism to extensional arc magmatism at 24 Ma in the Bocas del Toro Basin and Canal Basin areas (Fig. 2.1D). Farris et al. interpreted the geochemical switch to result from fracturing of the Panama arc block during initial collision with South America. Thus, Farris et al. suggested that the collision between Panama arc and South American Plate started at 24 Ma, and the collision caused the basin formation, normal faulting, and extensional magmatism in western Panama and the Canal area.

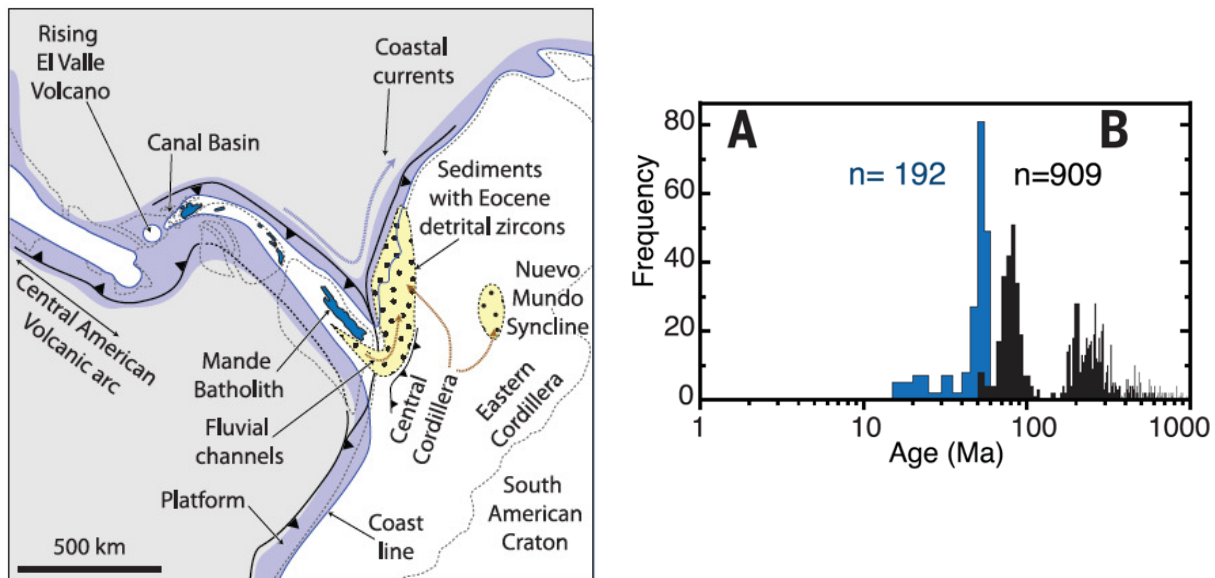


Figure 2.2 Paleogeographic reconstruction of the Panama arc block and northwestern South America during middle Miocene times. A and B zircon ages recovered from (A) lower Miocene strata in the Canal Basin and (B) Oligocene-Miocene strata in the Nuevo Mundo Syncline from Montes et al. (2015).

Montes et al. 2015 suggested an early closure age of the Central American Seaway using U/Pb detrital zircon geochronology on middle Miocene fluvial and shallow marine strata (Fig. 2.2). The paleogeographic reconstruction of the Panama arc and northwestern South America are

proposed to have occurred during middle Miocene times (15Ma to 13 Ma).

In contrast, Barat et al. (2014) proposed that the first contact of collision of southern Central America with South America occurred around 40Ma to 38Ma, and then propagated northwestwards. Barat et al. suggested that the horst and graben structures with thick sedimentary basin fills were caused by an extensional tectonic regime from the Middle Eocene to the Middle Miocene, and these geologic events are related to the collision between the central American arc block and South America.

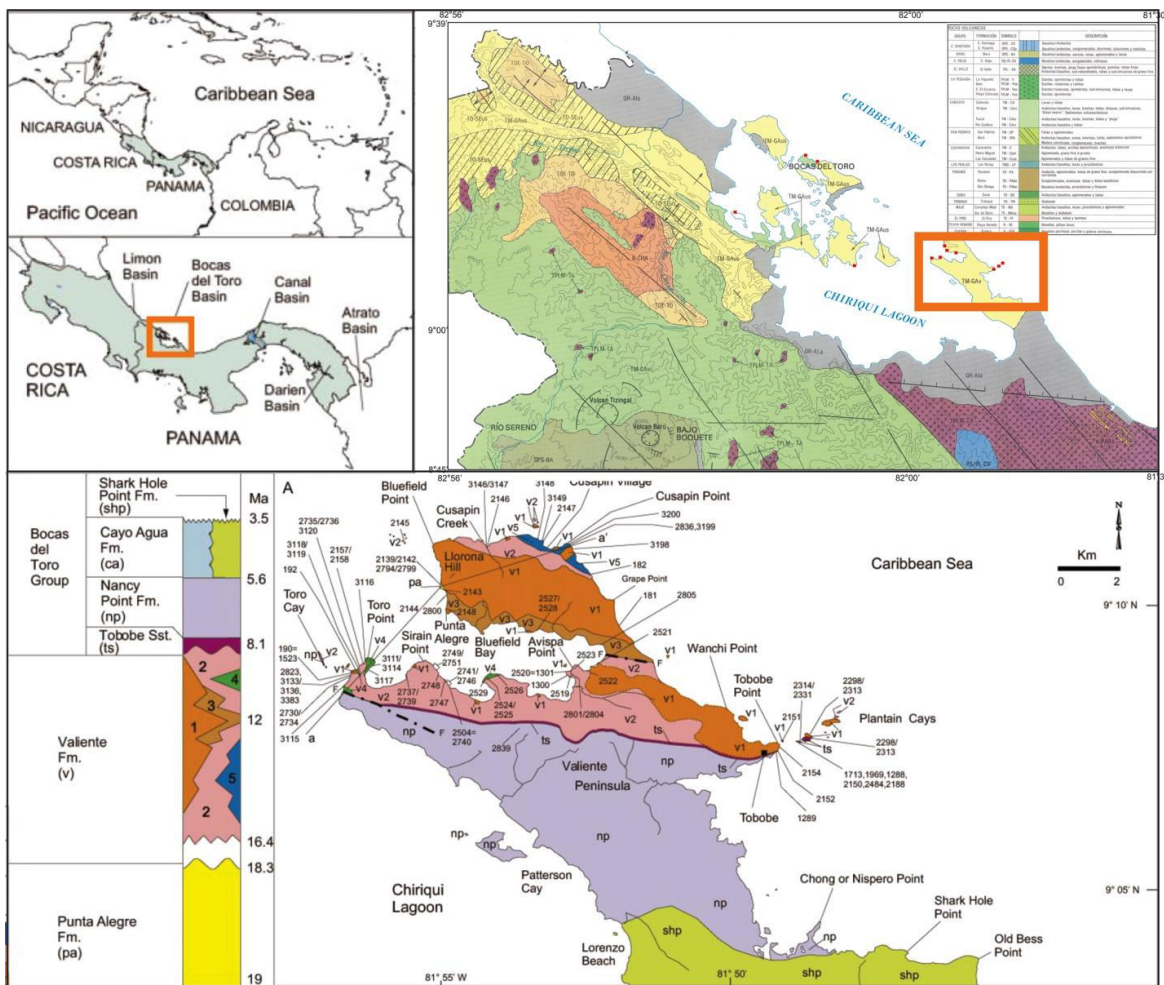


Figure 2.3 Simplified geologic map of the Bocas del Toro Basin, showing the sampling locations and the distribution of Punta Alegre and Valiente Formations in the Valiente Peninsula (Coates et al., 2003, 2005).

2.2 Stratigraphy and Volcanic Lavas in the Bocas del Toro Basin

The oldest sedimentary rocks in the Bocas del Toro Archipelago are from the early Miocene, about 20 Ma ago. The stratigraphic sequence records four phases in this archipelago, which are 1) Deposition of lower bathyal, oceanic sediments in early Miocene (21.5 Ma -18.5 Ma); 2) Volcanic arc basalts and basaltic andesites during middle Miocene (~18 Ma to ~12 Ma); 3) Extinction of the arc activities around 12 Ma and subsequent extensive emergence and erosion; 4) Subsidence of the volcanic arc during the latest part of Miocene time (~7.2 Ma -5.3 Ma) (McNeill et al., 2000; Coates et al., 2003, 2005).

The Bocas del Toro Archipelago can be divided into two main areas, northern and southern regions. The northern region comprises Swan Cay, Colon, Pastora, San Cristobal, Carinero and Bastimentos islands, and the Zapatillo Cays (Fig. 2.3). The Southern region comprises the islands of Popa, Deer, Cayo Agua, and Escudo de Veraguas, and the Valiente Peninsula. Generally, the northern region exhibits Pliocene-Pleistocene succession of shallow water sediments, especially coral reef deposits, and either unconformably overlies middle Miocene volcanic arc basalt or rest on the thick siliciclastic shale. The southern region reveals a more extensive volcanic arc suites of lower and middle Miocene rocks, which include deep-sea ooze, basalt and coarse volcanic sediments (Coates et al., 2003, 2005).

2.3 Ages of the Volcanic Lavas in Bocas del Toro

Coates et al. (2003) dated four samples of unaltered plagioclase phenocrysts from the coarse flow breccias sample (PPP2157, PPP2158) in the Toro Point of the Valiente Peninsula and one from a large dike (PPP2160, PPP2160) that intrudes the Valiente Formation in the south coast of Popa Island (Coates et al., 2003). The $^{40}\text{Ar}/^{39}\text{Ar}$ age spectrum for site PPP2157 in the Toro Point section yielded a plateau age of 11.88 ± 0.07 Ma, and the age spectrum for sample PPP2158, from the same flow as PPP2157, yielded a plateau age of 12.08 ± 0.07 Ma. The age spectra of plagioclase samples from sites PPP2060 and PPP2061, which are from the dike that intruded the Valiente Formation, yield two ages of 8.4 ± 0.4 Ma and 8.5 ± 0.5 Ma, respectively.

2.4 Lithology and Mineralogy

All the samples collected in Bocas del Toro come from the interbedded lavas (Fig. 2.4), and the lithology of these samples are trachy-basalt or trachy-andesite based on total alkali versus

silica (TAS) diagram (Fig. 4.2). Based on the petrographic studies of thin sections, these rocks are characterized by glassy and brecciated textures, and most of the recognized minerals in the matrix (80%) are plagioclase, amphibole, pyroxene, and some minor minerals, for example, biotite and feldspar. (Fig. 2.5) The mineralogical composition for the phenocryst phase is mainly plagioclase in the form of euhedral crystals. Pyroxene is the dominant ferromagnesian phase, but amphibole is also present. Slight post-alteration or weathering effects were observed during the microscopic studies due to contamination from coastal environment. The phenocrysts are surrounded by extensive glass in the matrix. This observation, coupled with the fact that the flows are interbedded with marine sedimentary rocks strongly suggests a submarine depositional environment.

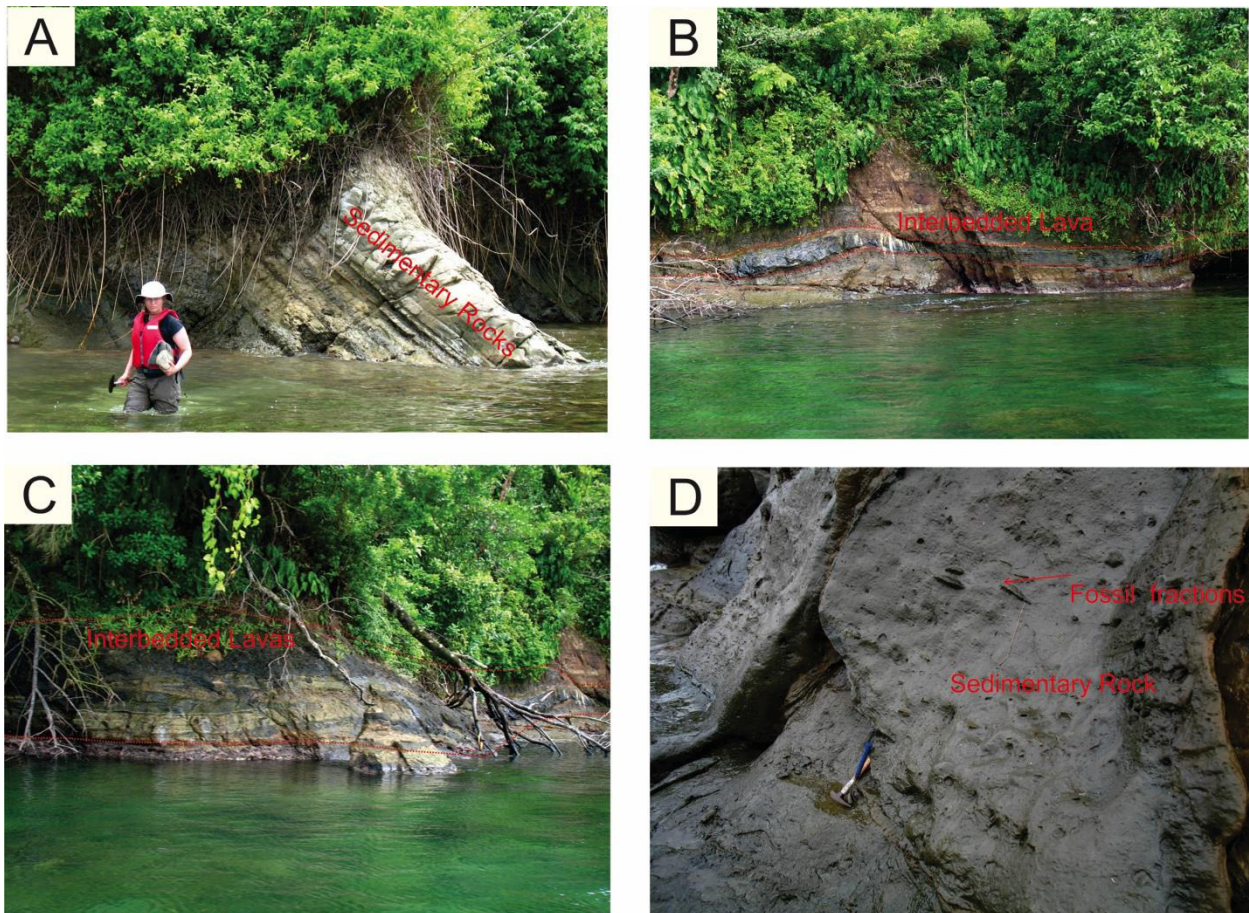


Figure 2.4 Field interbedded lava flows and sedimentary rocks formed in the coastal environment.

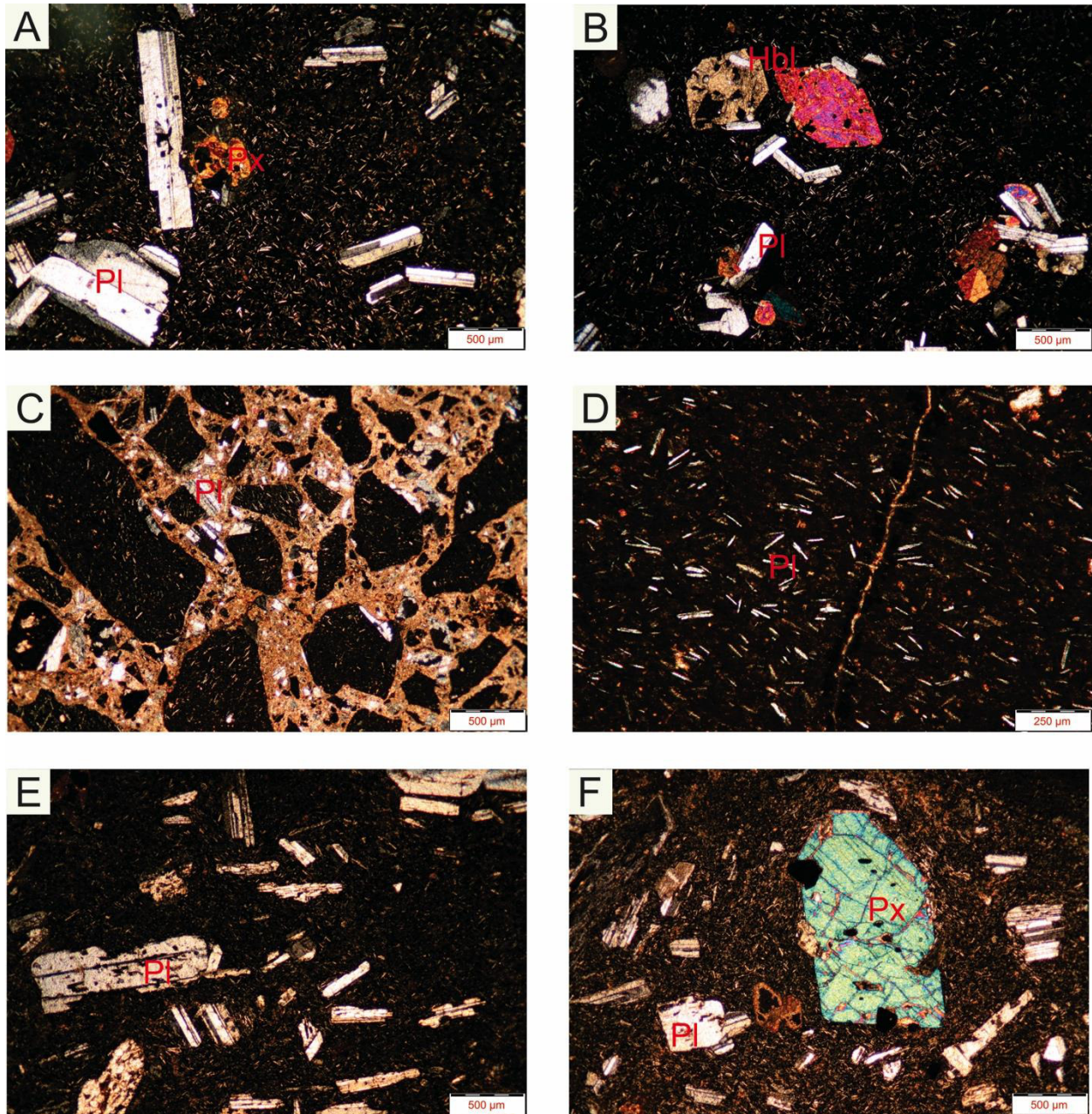


Figure 2.5 Microscopic pictures of the Bocos del Toro samples. Most of the samples present the porphyritic-like texture with ~80% matrix and euhedral plagioclase, pyroxene, amphibole, feldspar, biotite.

CHAPTER 3

ANALYTICAL METHOD AND DATA COLLECTION

3.1 Sampling and Data Collection

3.1.1 Sampling

A total of 13 sample locations were utilized, as shown in Figure 3.1. Most of the samples were collected in the Valiente Peninsula of the Bocas del Toro area, with other samples collected from Bastimentos island, Popa island and Pastores island. Columnar basalt flows and basaltic flow breccia make up most of the samples. All of the rocks sampled are interpreted to have depositional ages between 12-8 Ma based on the Ar-Ar geochronology (Coates et al., 2003).



Figure 3.1 Map of sample locations (six groups are illustrated in different icons and colors).

3.1.2 Data Collection

To conduct comparable analysis on the Bocas del Toro volcanic rocks, geochemical data

from previous workers has been aggregated and split into five Miocene and younger groups. Two important factors needed to be taken into consideration. The first is that the samples chosen should be andesite or basaltic andesite in composition, and should be Miocene or younger in age and have formed in an arc environment. Additionally, the selected samples are needed to come from adjacent Miocene arc sites with similar tectonic background (Abratis et al., 2001, Hidalgo and Rooney, 2010; Wegner et al., 2010; Farris et al., 2011, Hidalgo and Rooney 2014). Considering the diversity of the arc rocks and variations of geochemical composition, we divided all the data into five groups based on their chemical composition, arc background and tectonic constraints. The canal samples are also included in the study as its tectonic and magmatic background is similar to that of Bocas del Toro samples. These six groups are main arc tholeiite (~17-11 Ma) and calc-alkaline (~12-8 Ma), backarc alkaline (~8-2 Ma) and Bocas del Toro (~12-8 Ma), and adakite (< 2 Ma) groups and South Canal (25-15Ma) groups (Fig. 3.1).

3.2 Experimental Methods

Geochemical analysis of samples were done using instrumental neutron activation analysis (INAA) at the University of Missouri Research Reactor, while the XRF was conducted at the Smithsonian Museum Conservation Institute in Washington D.C. by Farris et al. (2011). During sample preparation, rocks were powdered using the agate mill to conduct the whole-rock elemental measurement. The analytical precision of INAA depends on the element and sample matrix. However, for most of the elements measured, the variation is less than 5 percent. See Farris et al. (2011) for a complete description of analytical methods.

CHAPTER 4

GEOCHEMISTRY

4.1 Major Element Chemistry

The lithology of the Bocas Bocas Del Toro volcanic lava flow mainly belongs to the category of trachy-basalt to trachy-andesite with the silicic composition ranging from 45 weight percent to 64 weight percent (wt. %) (Fig. 4.1). Comparing them with other group samples, the Bocas del Toro rocks are more silicic in terms of silicic composition. The MgO composition is much lower when compared with other five groups as mentioned above, ranging from 0.35 wt. %-3.43 wt. % and those values are lower than $MgO=30-0.43*SiO_2$ trend in the MgO v.s. SiO₂ plot (Smith et al., 1997) (Fig. 4.1), which means these samples were not fully crystallized products from primary magma without any crustal contamination or interruption from the original magma. The low MgO and high-SiO₂ composition in the samples also refers to the high degree of crystallization from the primary magma.

In comparison with the tholeiite, calc-alkaline, backarc alkaline and adakite group samples, the Bocas del Toro basin samples exhibit lower slope trend (MgO/SiO₂) and lower values of MgO when compared with other samples of the same silicic content (Fig. 4.1). However, the Bocas del Toro group samples show the highest value of potassium (K₂O) (except for samples of 070111 and 070117 with relative lower values). This geochemical signature makes the Bocas del Toro rocks fall into the category of shoshonite series in the K₂O vs. SiO₂ plot, which can distinguish this group from most of the other ones (Fig. 4.3). However, the back-arc alkaline group is most similar in terms of composition. Through the AFM diagram, the Bocas del Toro rocks exhibit calc-alkaline igneous characteristics, and show similar features to the backarc alkaline and calc-alkaline group (Fig. 4.4A). The diagram of FeOt/MgO vs. SiO₂ also supports the grouping concept of tholeiite and calc-alkaline rocks (Fig. 4.4B). The Bocas group exhibits a little depletion of FeOt (all Fe as FeO) with a range of 3.9-8.0 wt. %, which is relatively lower in value and has smaller slope than most of other group samples, especially when comparing it with the tholeiite group. The major element CaO content is also a little lower relative to other groups, whereas the trend of CaO vs. SiO₂ plotting slope is the same as other group samples.

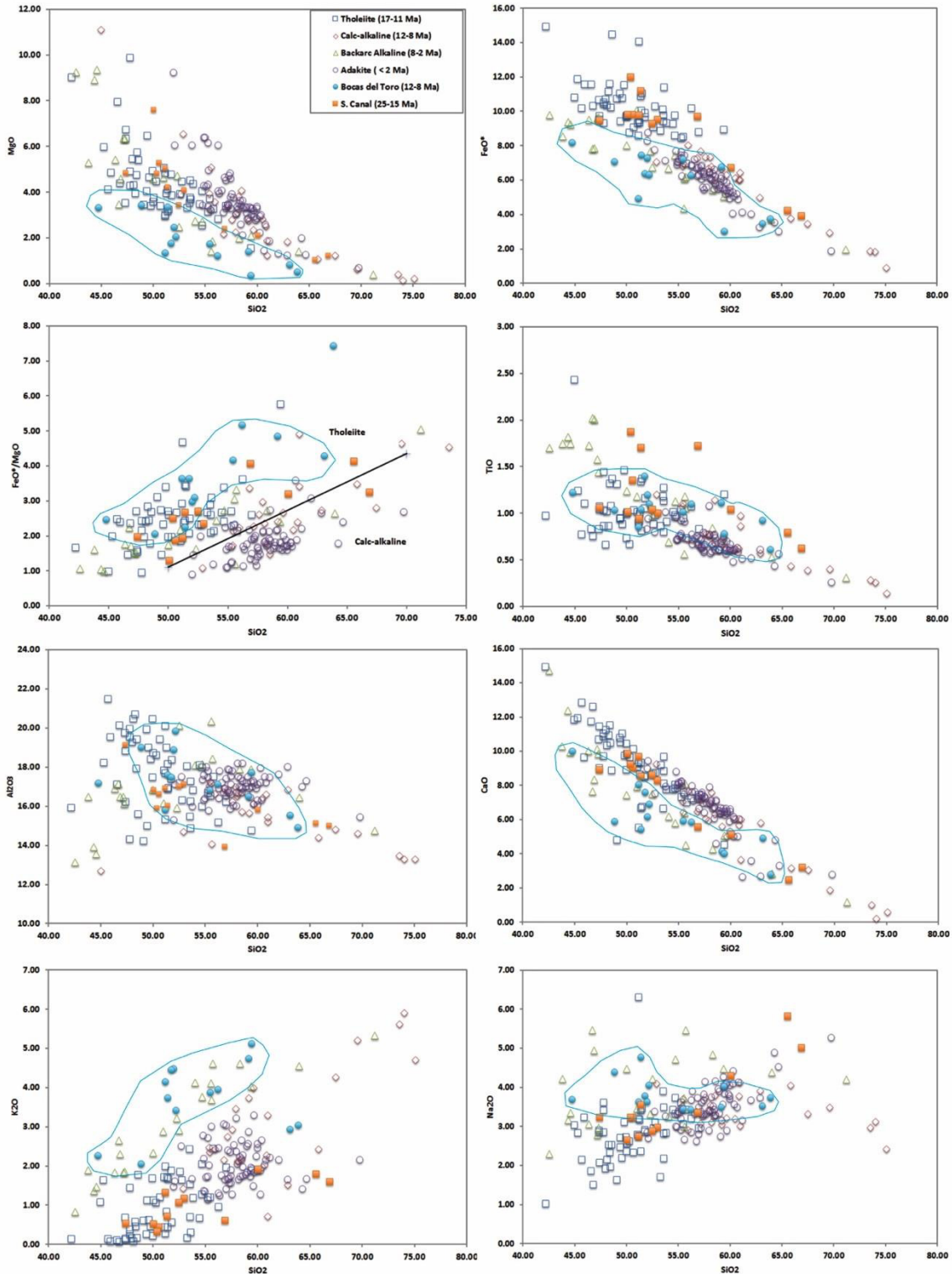


Figure 4.1 Major element chemistry of the Bocas del Toro rocks. The tholeiite, calc-alkaline, backarc calc-alkaline, adakite and Canal samples are plotted for data background, and their references and sampling locations can be found in Chapter 3 (Abratis et al., 2001; Hidalgo and Rooney, 2010; Wegner et al., 2010; Hidalgo and Rooney, 2014).

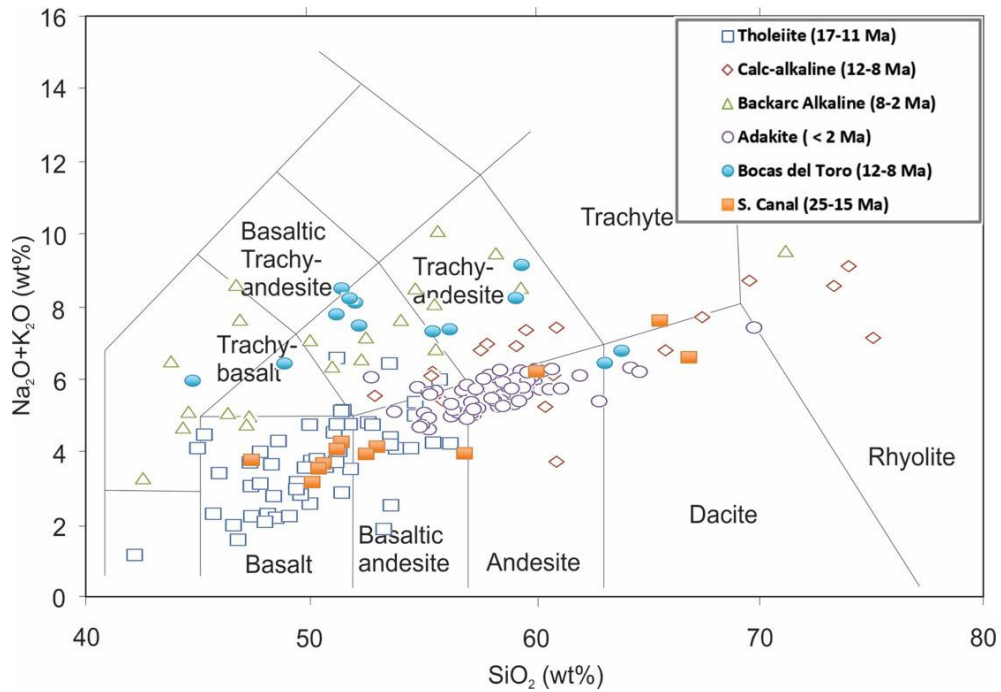


Figure 4.2 Chemical classification and nomenclature of volcanic rocks displayed in total alkali vs. silica (TAS) diagram according to Le Maitre et al. (1989) and Le Bas et al. (1991).

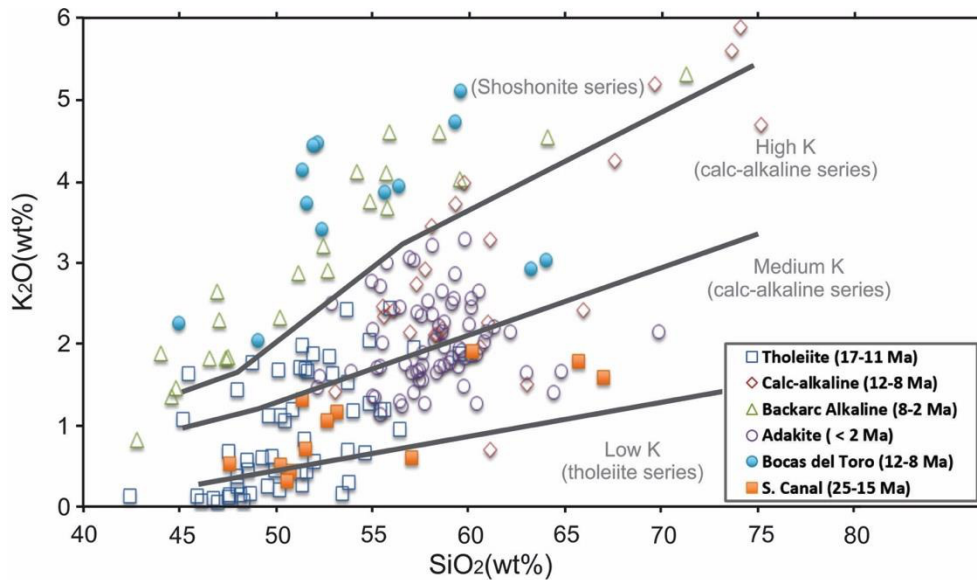


Figure 4.3 Subdivision of subalkaline rocks after Rickwood (1989) based on the basis of K_2O vs. SiO_2 .

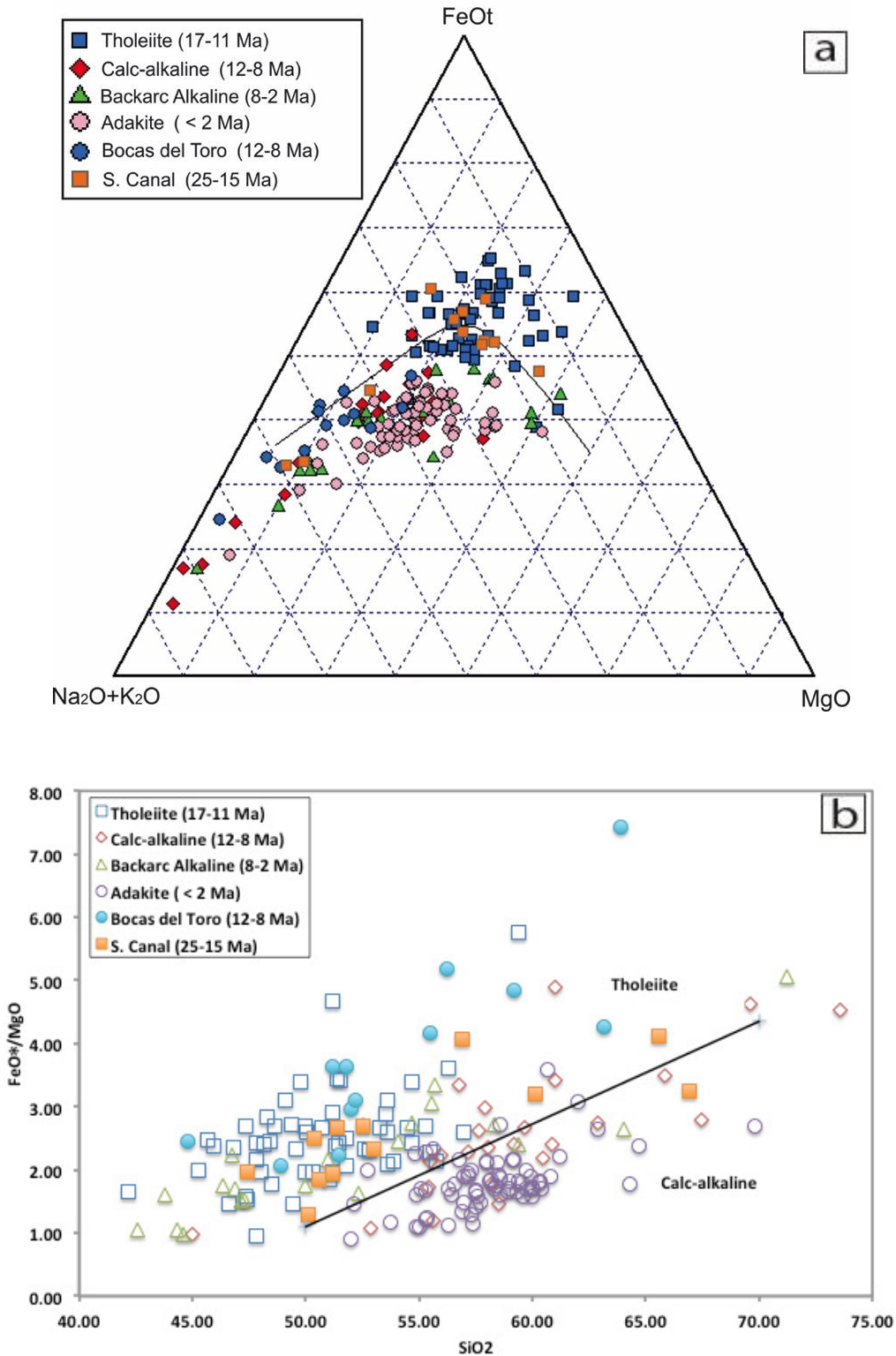


Figure 4.4 a. AFM diagram for the tholeiite and calc-alkaline evolution series (Thompson, 1976); b. FeO*/MgO vs. SiO₂ diagram shows that the rocks can generally be divided by the tholeiite and calc-alkaline boundary.

4.2 Trace Element Chemistry

By plotting the trace elements from Bocas samples normalized to primitive-mantle normalized spider diagram, it's easy to show that all the group samples show clear arc chemical signature with a low Nb and Ta contents, exhibiting relative enrichment in fluid-mobile large ion lithophile elements (LILEs) (Fig. 4.5), and all groups have obvious Ti negative anomaly. However, the calc-alkaline, backarc alkaline and Bocas del Toro basin groups have no clear Sr positive anomaly as occurred in other group rocks. But, in comparison with rocks from the other groups, the Bocas del Toro rocks have a significantly decreased Ta anomaly, and mostly relative higher Nb content (Nb > 20 ppm). Compositionally, high-Nb basalts are similar to HIMU (high U/Pb) ocean island basalts, continental alkaline basalts and alkaline lavas formed above slab windows or mixed with a small amount of OIB-source materials (Hastie et al., 2011).

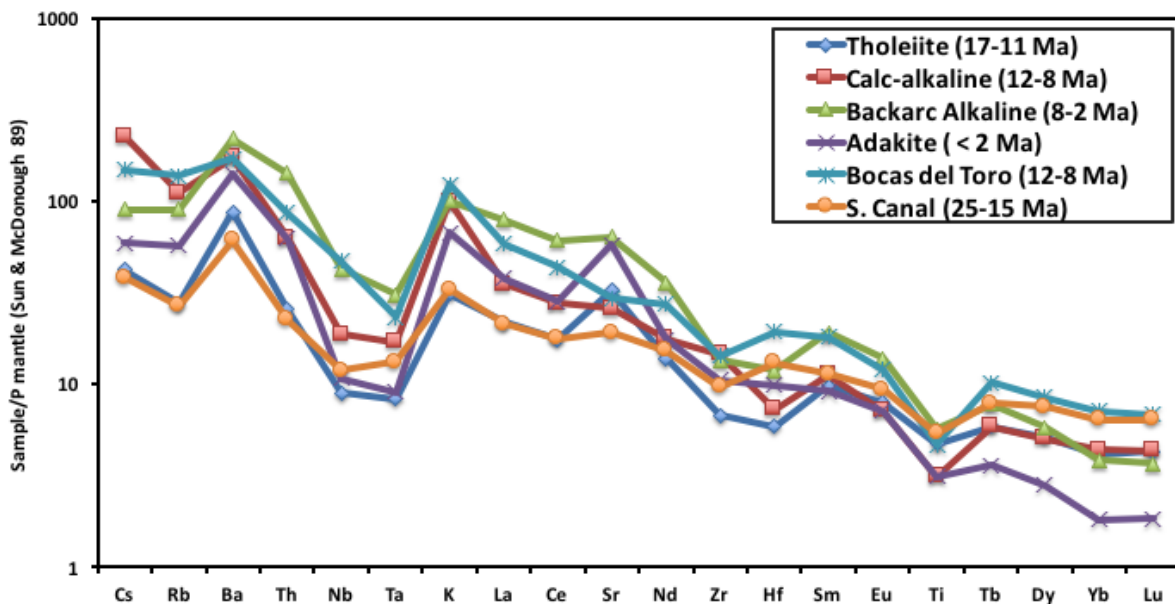


Figure 4.5 Trace element patterns of the different group components.

Plotting of the tectonic discrimination diagrams can provide more information about tectonic background (Fig. 4.6). The Hf/3-Th-Ta diagram shows that most rocks from the five groups fall into the volcanic arc basalts area, which corresponds with the trace element spider diagram. Few samples fall in the within plate tholeiite and alkaline within plate basalt area, which means for certain samples or groups, their formative environment is different relative to Bocas del

Toro group rocks.

This Ta/Yb vs. Th/Yb diagram can be used to recognize arc magmas generated through subduction and fluid enrichment of a depleted to enriched mantle sources. All trace element ratio plots show that Bocas del Toro rocks host a moderate enriched OIB-signature, and are transitional from the older tholeiitic group to the youngest adakites. The Cocos Ridge samples were also included on the plots to determine possible linkages in their genetic background. The Cocos track rocks are melting products of the Galapagos hot spot, which is an active plume in East Pacific Ocean. By putting them in a same diagram, it shows that the Bocas del Toro samples inherit parts of their chemical characteristics from the enriched subducted slab and show clear enriched OIB signature (Ta, La, Th, etc). The Bocas del Toro samples also have the closest and lowest value of (Ba/La)/N value with that of the Cocos tracks, and combined with the low value of Sr and the ages of the Bocas del Toro arc rocks and the colliding Cocos track, the enriched signal in the Bocas del Toro arc rocks possibly originate from the melting of the subducted slab or from influx of the Galapagos mantle via a slab window (Figure 4.7 B, C and D) (Eiler et al., 2005).

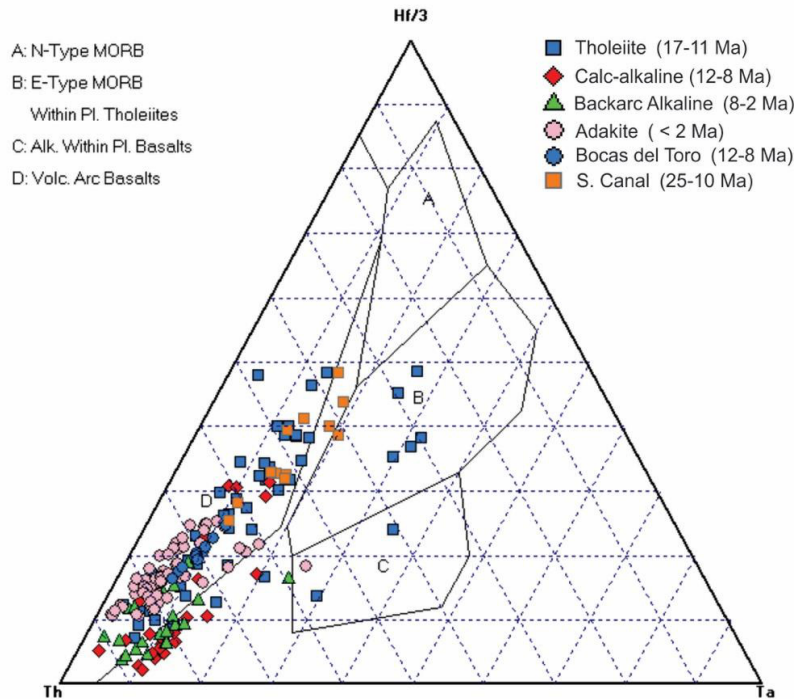


Figure 4.6 Hf/3-Th-Ta diagram (Wood, 1980).

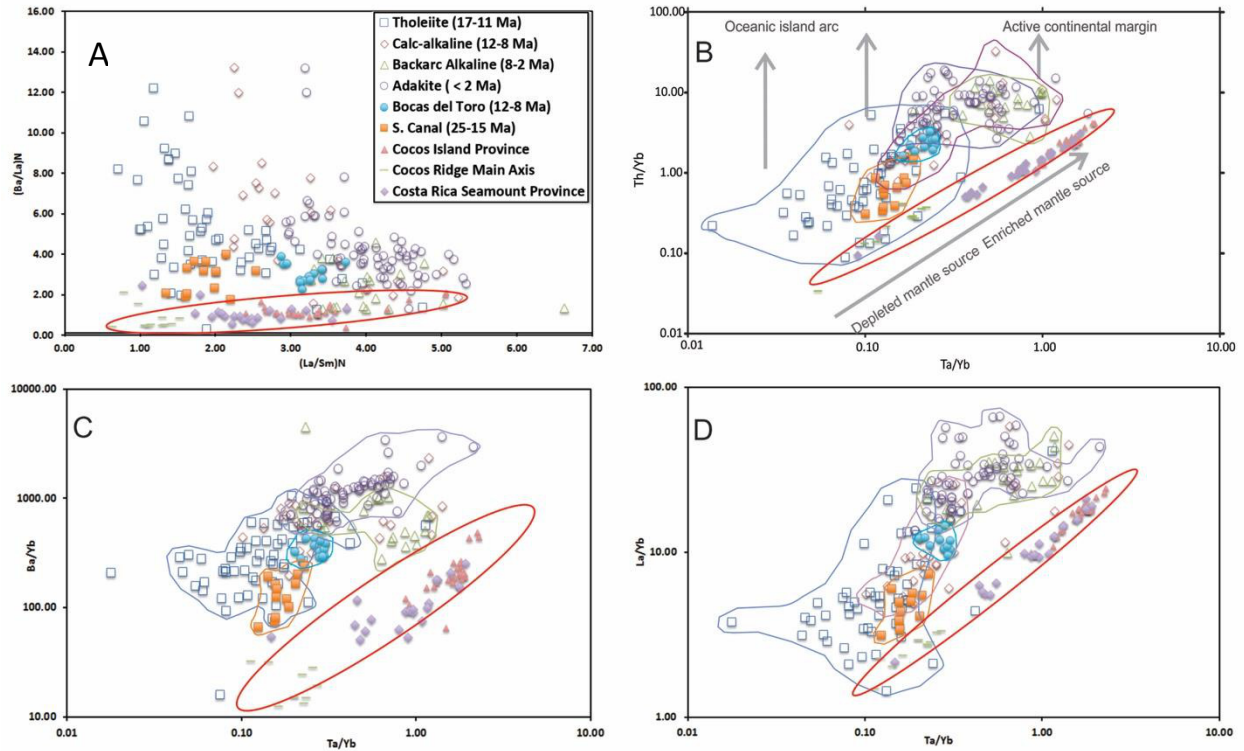


Figure 4.7 A. (Ba/La)_N vs. (Ta/Sm)_N diagram; B. Th/Yb vs. Ta/Yb diagram; C. Plot of Ba/Yb vs. TA/Yb for magmatic rocks; D. La/Yb vs. Ta/Yb diagram. The red circles represent the Cocos track distributing area.

4.3 Isotope Geochemistry

4.3.1 Pb-Nd Isotopes

As the tracks of the Galapagos hot spot, both of the Cocos Ridge/Coiba Ridge (central Galapagos Domain) and the Seamount Province (Northern Galapagos Domain) host strong, anomalous, enriched geochemical signatures (Fig. 4.8) (Gazel et al., 2009; Herzberg and Gazel 2009).

The isotopic data from the tholeiite (17-11 Ma), calc-alkaline (12-8 Ma), backarc alkaline (8-2 Ma), adakite (< 2 Ma) were plotted in an isotopic diagram (Fig. 4.8), and shows that the younger rocks have relative stronger enriched geochemical signature of OIB. However, the adakite group crosses the Cocos Ridge/Coiba Ridge and Seamount Province plotting areas. The backarc alkaline rocks fall into the Cocos Ridge/Coiba Ridge (central Galapagos Domain). Even

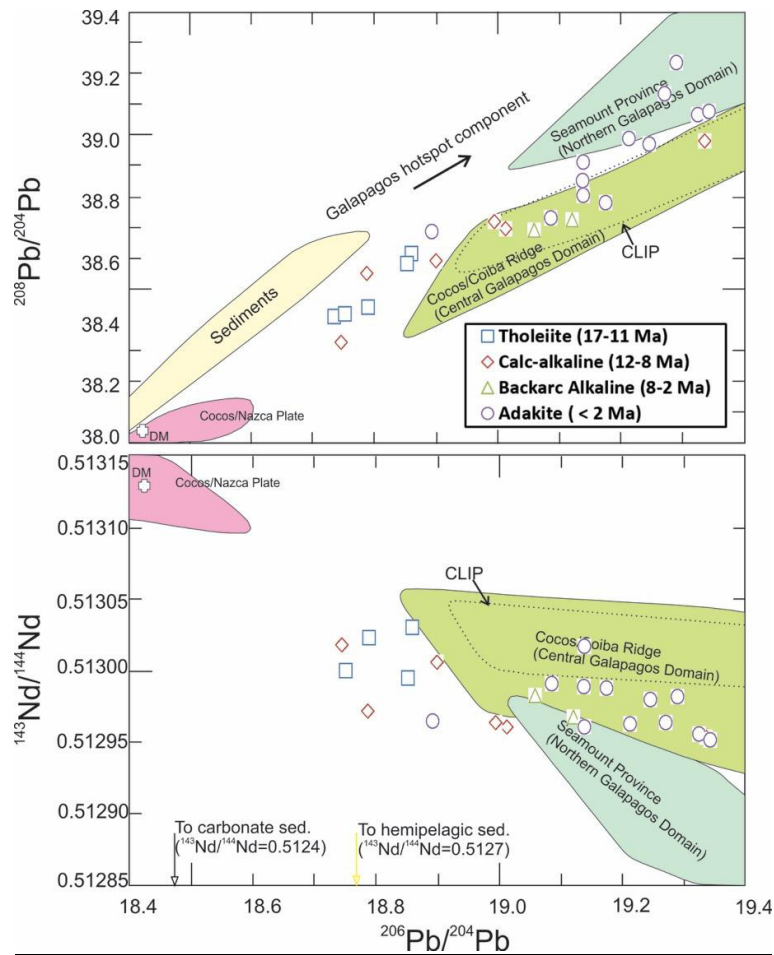


Figure 4.8 Pb and Nd isotopic ratios for samples of the Oligocene-Pliocene samples, the central Costa Rican and Nicaraguan volcanic front lavas, and alkaline basalts and adakites from Costa Rica and Panama. Data background from Gazel et al., 2009. Hoernle et al. (2000), Werner et al. (2003) and Feigenson et al. (2004).

though the tholeiite and calc-alkaline groups fall outside of the Cocos Ridge/Coiba Ridge and Seamount Province areas, their evolution trend seems it is approaching to the two enriched areas. It can be concluded that an OIB-like component mixed into the initial melts in the mantle wedge, which occurred at least before the volcanic magmatism of the tholeiite and calc-alkaline rock groups.

It is believed that the isotopic values on our studying area should be distributed in the area closing to the calc-alkaline and backarc alkaline groups for the following two reasons: 1) Based on the diagrams of diverse trace element geochemistry, all the Bocas del Toro samples fall between the two groups mentioned above; 2) With the evolution of arc magmatism, and more

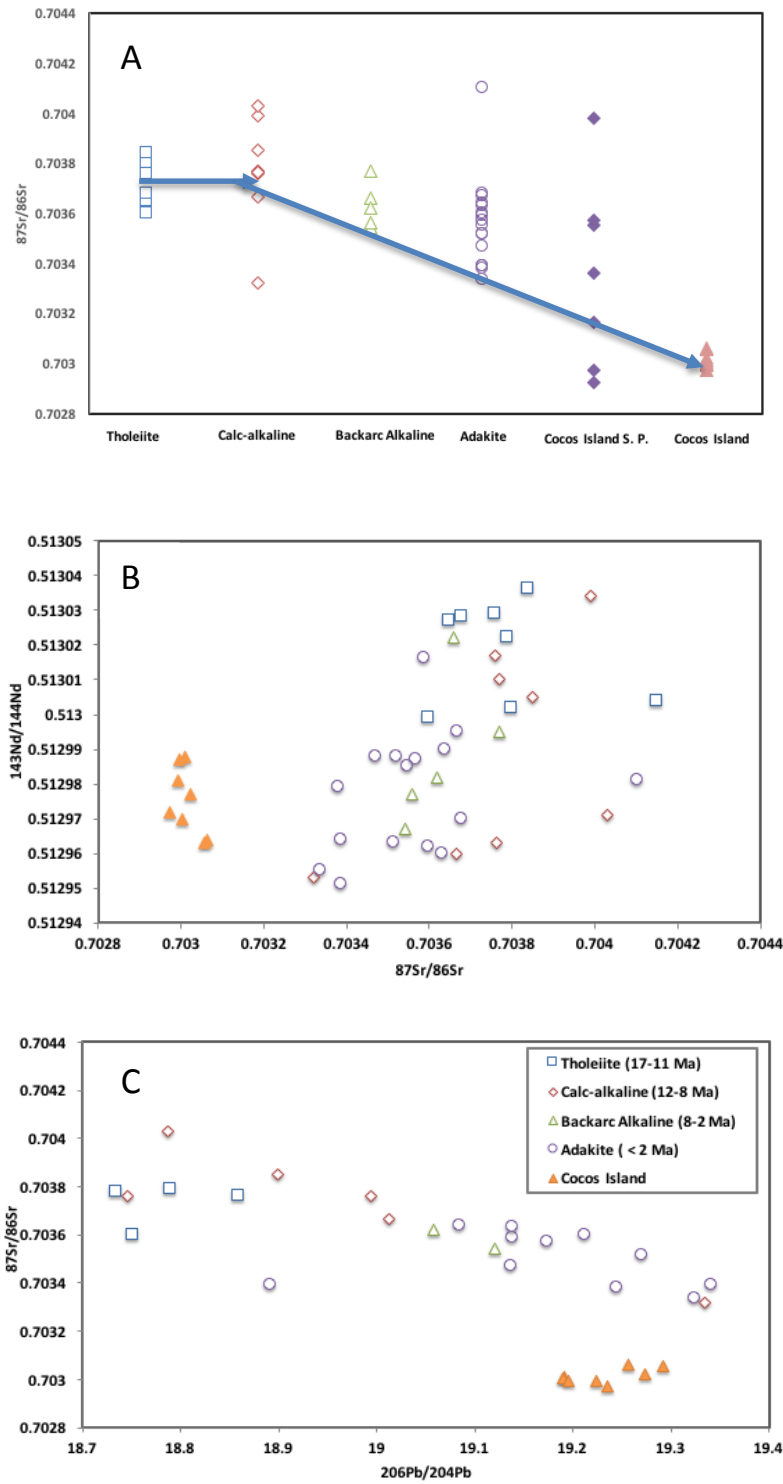


Figure 4.9 Sr-Nd-Pb isotope diagrams. A. $^{87}\text{Sr}/^{86}\text{Sr}$ vs. tholeiite, calc-alkaline, backarc alkaline, adakite and Cocos island diagram; B. $^{143}\text{Nd}/^{144}\text{Nd}$ vs. $^{87}\text{Sr}/^{86}\text{Sr}$ diagram; C. $^{87}\text{Sr}/^{86}\text{Sr}$ vs. $^{206}\text{Pb}/^{204}\text{Pb}$ diagram.

and more Galapagos enriched component mixed into the melts, the younger arc volcanic rocks show a higher percentage of OIB-like components. Therefore, we assume that the isotopic data of the Bocas del Toro rocks generally will fall into the area between the calc-alkaline and backarc alkaline groups. In this case, we can generally conclude that the Bocas del Toro rocks also show an enriched geochemical signature. Isotopic analysis of the Bocas del Toro volcanic rocks is a goal for future research. However, this assumed conclusion still can be used in the following isotope models.

Fig. 4. 9 illustrates that with continued evolution of arc magmatism, the ratio of $^{87}\text{Sr}/^{86}\text{Sr}$ generally keeps decreasing from the tholeiite and calc-alkaline groups, from the highest average value of $^{87}\text{Sr}/^{86}\text{Sr}$ (0.7038) to the lowest average value of $^{87}\text{Sr}/^{86}\text{Sr}$ (0.7030). By comparing the diagrams of $^{143}\text{Nd}/^{144}\text{Nd}$ vs. $^{87}\text{Sr}/^{86}\text{Sr}$, $^{87}\text{Sr}/^{86}\text{Sr}$ vs. $^{206}\text{Pb}/^{204}\text{Pb}$, the diagrams show that more enriched geochemical components and deeper materials mixed with the mantle wedge melts, especially as featured in the younger arc rocks.

CHAPTER 5

GEOCHEMICAL MODELS

Modeling the Bocas del Toro arc magmatic processes, including the partial melting of the mantle wedge and fractional crystallization is the necessary method to reveal its conditions and processes of formation. The models can also place quantitative constraints on the pressures and temperatures of melting and crystallization. For major element modeling the MELTS Software (Gualda and Ghiorso, 2015) is used to simulate the process of fractional crystallization, and the backward calculation trace distribution coefficient element method and the ARC BASALT SIMULATOR 3.0 (Kimura et al., 2010) were used to simulate melting processes and to constrain formative conditions and source contributions in the mantle wedge.

5.1 Fractional Crystallization Model

5.1.1 Parameters of the Modeling

To determine the conditions of formation of the Bocas del Toro arc volcanic rocks, the MELTS program (Gualda and Ghiorso, 2015) was employed to model the process of fractional crystallization. As all Bocas samples have very low magnesium content (MgO), ranging from 0.35 wt. % -3.43 wt. %, which suggests the Bocas del Toro samples are the end products from the crystallization of a primary magma and may have mixed with a limited component. Samples such as these are not ideal starting composition. So, none of samples in the Bocas area can be used as the initial composition. All samples which share similar genetic background to the Bocas del Toro rocks were examined by selecting the samples which show the closest relatives with the primary magma with regard to high MgO concentrations, highest Mg# ($100\text{Mg}/(\text{Mg}+\text{Fe})$), low SiO₂ and relative higher in Ni, Cr concentration. Those showing the closest geologic age and sharing similar tectonic backgrounds are also important when selecting the starting sample candidates. By taking all the factors into consideration, GUA 33 (MgO 8.91 wt. %), GUA 27 (MgO 9.25 wt. %), PAN-06-039 (MgO 11.10 wt. %) and PAN-06-052 (MgO 9.88 wt. %) (Wegner et al. 2010; Abratis et al., 2001) were chosen as our magma composition, and GUA 33 and PAN-06-039 are relatively better samples to be put in the Melts Program. 1.0-5.0 wt. % H₂O was added into the original starting composition respectively, and it concludes that different percentages of water do not have

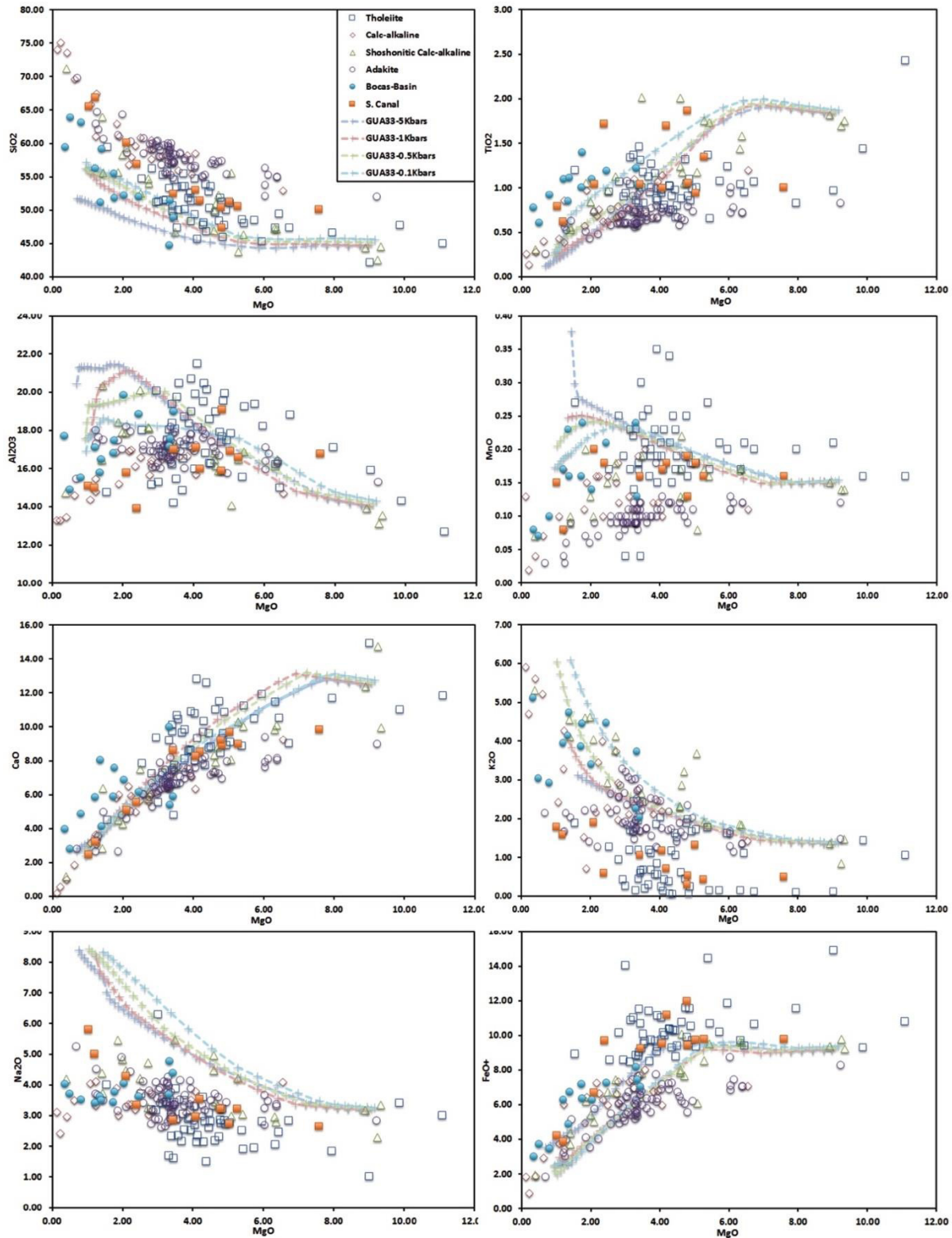


Figure 5.1 GUA 33 MELTS major element modeling of different groups of volcanic rocks with 0.1, 0.5, 1.0, and 5.0 kbars in pressure.

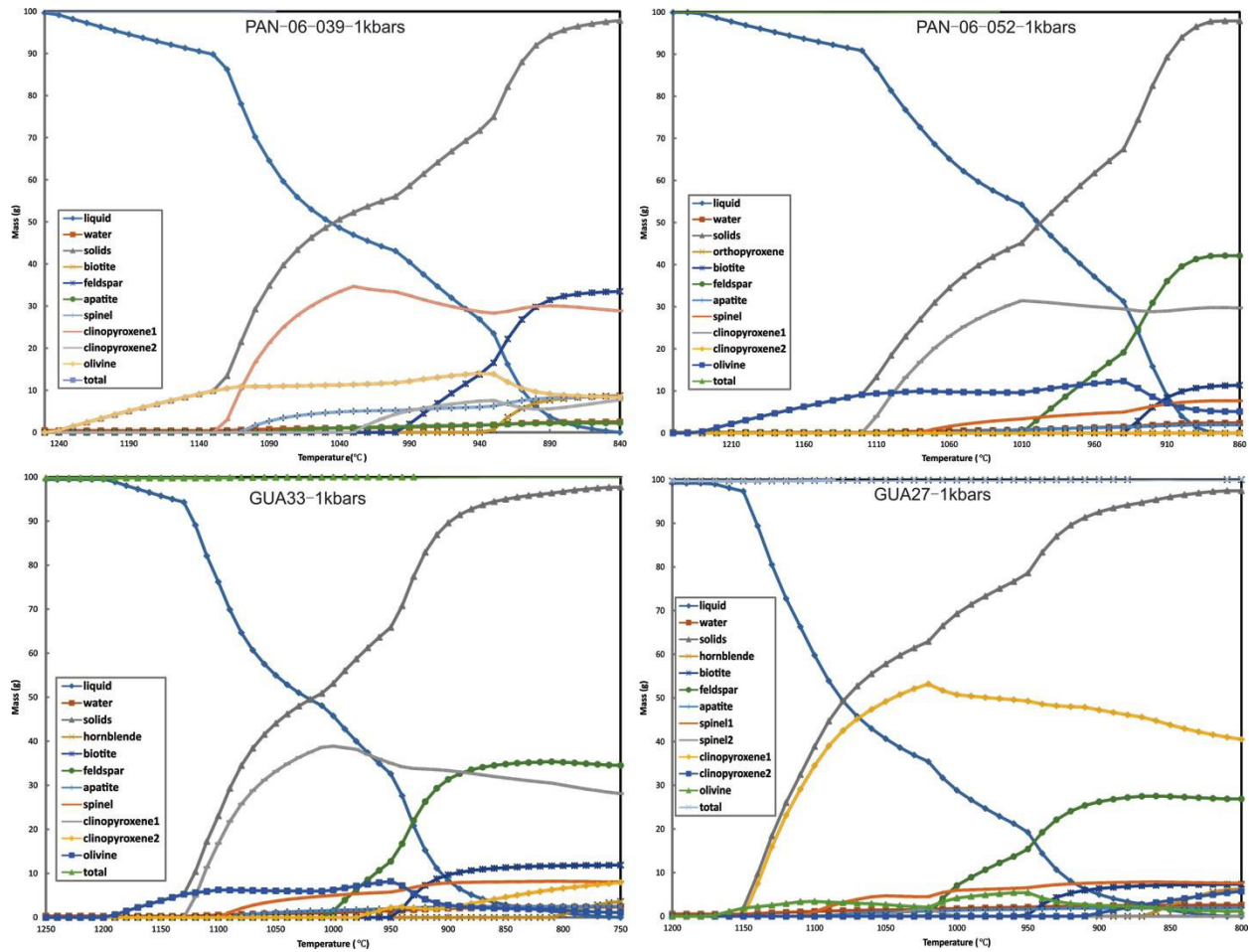


Figure 5.2 Mass and mineral crystallization curves for GUA 33, GUA 27, PAN-06-039 and PAN-06-052 in 1kbars pressure.

a significant effect on fractional crystallization and its products. However, among them 3 wt. % H₂O content works best as a water constraint and also is in accordance with the arc geologic processes. All models were run decreased in temperature from 1350° to 700° C in 10° increments, and in the pressures of 10, 5.0, 1.0, 0.5 and 0.1 kbar, respectively. Ni-NiO oxygen fugacity buffers were selected to be the operating oxygen status.

5.1.2 Outcome of the Modeling

Pressure condition during crystallization is the most important factor affecting the liquidus temperature and the formation order of minerals in this specific geologic example. Fractional crystallization modelling runs using GUA 33 and PAN-06-039 as a starting composition, which

corresponds best with observed compositional data (SiO_2 - MgO , - Al_2O_3 , - Ti_2O , - FeO^* , - K_2O , - CaO , - MnO) when the pressure is around 1kbar (Fig. 5.1). However, one exception is that Na_2O doesn't fit in to the modeling very well due to the extreme low content of Na_2O . The minerals started to crystallize around 1200 ° C to 900° C as plotted in the diagrams.

The Melts modeling suggests that the samples GUA 33 need 55% fractional crystallization to evolve from the starting composition to main area of most Bocas del Toro rocks (Fig. 5.2). Therefore, if the samples crystallize from a primary magma, it will require a high degree of fraction. Detailed analysis of the crystal fractionation extent will be examined to deduce the composition of the primary magma trace element concentrations.

5.2 Isotopic and Trace Element Partial Melting Model

To estimate the regional and temporal contribution of mantle wedge (MW), slab altered oceanic crust (AOC) and the uppermost sediments in the slab (SED) to the arc magmatism in Bocas del Toro, we employed three methods to model the partial melting processes.

5.2.1 Isotopic Element Model

Multiple isotopes were used to constrain the contribution of OIB-like components to the mantle wedge melts. For this thesis, even though we have no isotopic data on the Bocas del Toro samples, we infer its isotopic composition to be between the general calc-alkaline and the backarc alkaline groups depending on its ages and the evolution of trace elements. In this case, as shown in the Fig. 5.3, the contribution originating from the Galapagoes hotspot should be between 1% and 3%. 1.5% was used as the operating value of chemical modeling when mixing different percentages of the end members.

5.2.2 Trace Element Model #1

The first step for modeling the partial melting is to quantify the three end member compositions: the mantle wedge (similar to depleted mantle (DM)), AOC and upper crustal sediments. The mantle wedge composition in this model is calculated using Gazel's (Gazel et al., 2009) method by inverting a melt fraction of 8% of the sample SO-144-1 (A. Table 3) from the EPR-Cocos crust off Nicaragua (Werner et al., 2003). This calculated DM composition here is similar

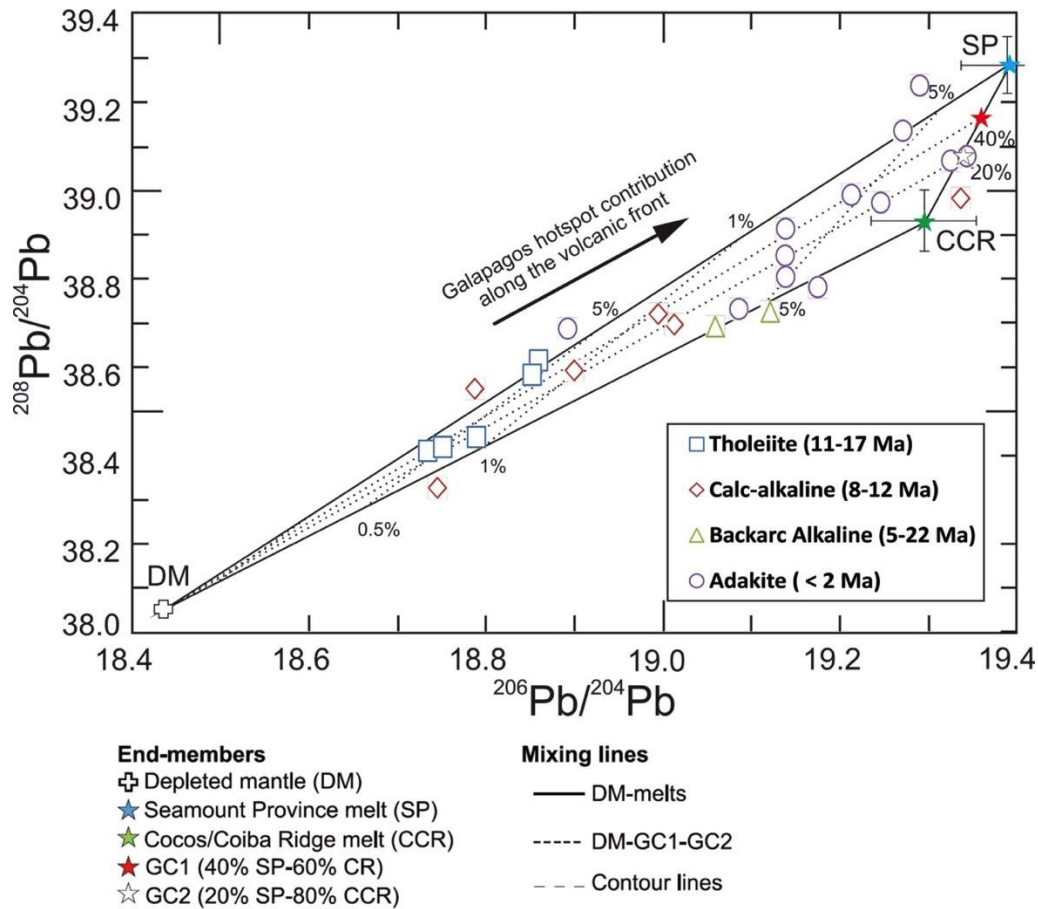


Figure 5.3 Mixing lines connecting the modeled mean Seamount Province melt ($^{143}\text{Nd}/^{144}\text{Nd}=0.51286$, $^{206}\text{Pb}/^{204}\text{Pb}=19.390$, $^{208}\text{Pb}/^{204}\text{Pb}=39.284$) and the mean Cocos/Coiba Ridge melt ($^{143}\text{Nd}/^{144}\text{Nd}=0.51297$, $^{206}\text{Pb}/^{204}\text{Pb}=19.296$, $^{208}\text{Pb}/^{204}\text{Pb}=38.930$) (Hoernle et al., 2000; Werner et al., 2003) with the DM (inverted from sample SO144-1) from Werner et al. (2003). Revised from (Gazel et al., 2009).

in the trace element composition to that reported by (Workman and Hart, 2004). It's assumed that the enriched component comes from the Cocos Ridge, the tracks of the Galapagos hotspot. Here, the OIB contributions were modeled from the mean values of the subducted Seamount Province and the Cocos/Coiba Ridge reported by (Hoernle et al., 2000) and (Werner et al., 2003) using 20% melting in the eclogite facies. The final components are two sedimentary melts based on the sediment compositions of (Patino et al., 2000) with a melt fraction of 20% (Gazel et al., 2009). Pr and Ta, not included in the original data, were calculated from adjacent elements which share similar geochemical features normalized to Sun and McDonough (1989) values. The sediment melt used in the trace element model consists of a mix of 30% mean carbonate and 70% mean

hemipelagic sediments (Gazel et al., 2009).

The melting model used in this study is aggregated fractional melting (Shaw, 1970) described by the equation of $C_L/C_0 = 1/F * [1 - (1 - F)^{1/D_0}]$, and the partition coefficients used in our modeling are from the Geochemical Earth Reference Model website and Rollinson et al. (1993) and the compilation of (Kelemen et al., 2003) (A. Table 3). Where C_L is the average concentration of the element in the liquid, C_0 is the initial concentration of the element in the source, F is the melt fraction, and D_0 is the initial bulk partition coefficient. The equation is derived from the mass balance equation $C_0 = F * C_L + (1 - F) * C_S$, and the bulk partition coefficient $D = C_S/C_L$. Where C_S is the concentration of the element in the solid phase.

Different percentages of the three end-members were mixed and calculated by different partial fraction, $F=2\%$, 5% and 8% . When 0.5% sediment and 1.5% OIB were mixed into the mantle wedge with a melting fraction of $F= 5\%$, we can produce the Bocas del Toro primary magma (Fig. 5.4A). As the current Bocas del Toro trace elements have experienced fractional crystallization, we get the partial fraction value when the modeled Ta value matches the smallest Ta value in the Bocas del Toro sample. Based on the model, 1.5% OIB-signature enriched geochemical component mixed into the localized mantle wedge. The depleted mantle or the magma source experienced around 5% of partial melting in this model.

5.2.3 Trace Element Model 2

The enriched chemical pattern of the Bocas del Toro rocks and other similar groups can also originate from an OIB-like mantle wedge, which is assumed to be enriched by the Galapagos plume. Herrstrom et al. (1995) suggested that Costa Rican lavas are derived from a part of the mantle wedge showing the sources of certain ocean-island basalts (OIB). In this trace element model, the properties of the “OIB-like” mantle wedge component are based on the assumption that sample T24-2 from Turrialba (the best-characterized, high-La/Sm) is a 5% batch partial melt of that source (Eiler et al., 2000, 2005). As described above, the key feature of these models is that the mantle wedge is assumed to be metasomatized by variable amounts of two slab-derived components: The first is meant to approximate a partial melt of sediments from the uppermost top of the slab, and it has a $\delta^{18}\text{O}$ value of $+25\%$ with a water content of $10 \text{ wt.}\%$. The second one is meant to approximate an aqueous fluid derived from dehydration metamorphism of hydrothermally altered gabbros and/or serpentinites in the slab interior, and it is assumed to have

a $\delta^{18}\text{O}$ value of 0%.

In this modeling, the same equation and the same partial melting coefficients in the first model were used (Fig. 5.4B). In model # 2 we gain a very similar outcome to model #1. The partial melting fraction is about 5% and with the mixture contribution of 99% ‘‘OIB-like’’ mantle wedge component, 0.5% low- $\delta^{18}\text{O}$ value component and 0.5% High- $\delta^{18}\text{O}$ value component, which corresponds with the first model.

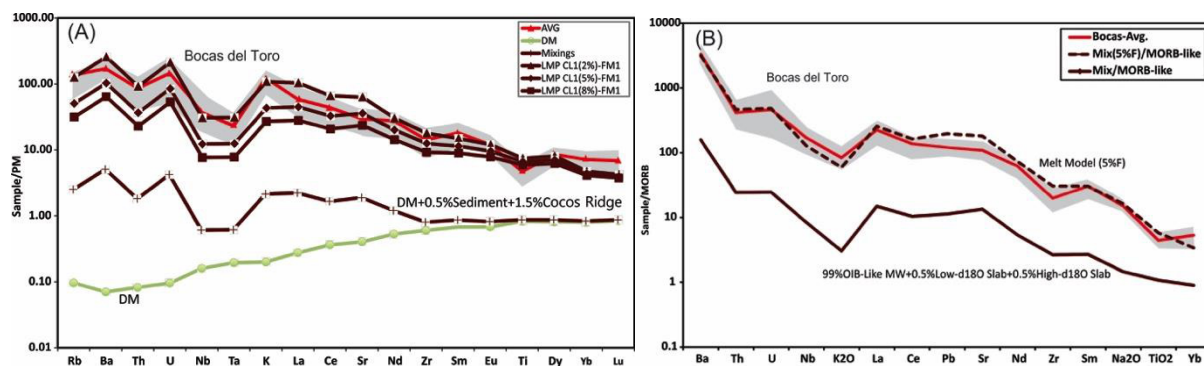


Figure 5.4 A: Model #1, and B: Model #2 for partial melting processes.

5.2.4 Arc Basalt Simulating

We selected 6 samples from all the analyzed samples and employed software of Arc Basalt Simulator version 3 (ABS3) to examine the mass balance of slab dehydration, partial melting, slab fluid/melt-fluxed mantle melting and to quantitatively evaluate magma genesis (Kimura et al., 2010). We present major and trace element data for the Bocas del Toro arc rocks, which show chemical outcomes consistent with the two trace element models above (#1 and #2) (Fig. 5.5). Our procedures for simulating the partial melting is as followed:

Step 1: As the samples collected in the Bocas area are too silicic and have low MgO concentration, the depleted mantle information of the primary melts can't be gained by inferring from Bocas del Toro samples. Therefore, three end-members were chosen from the dataset, and uppermost sediments and interior altered slab come from Gazel's dataset (Gazel et al., 2009). By replacing the original dataset from the ABS3 software with our own data we can, to the largest extent, model the geologic facts and obtain the most exact condition parameters.

Step 2: By inverse calculation, the primary trace elements information for the primary

magma in Bocas del Toro rocks can be obtained, and PRIMELT 2 software (Herzberg and Asimow, 2008) was employed to obtain the primary values for the major elements (Rooney and Deering, 2013). Primary magma information is used to determine the crystallization fraction from the primary magma to the current Bocas del Toro igneous rocks. By using the MELTS program (Gualda and Ghiorso, 2015) the percentage was received, which is about $F = 60\%$. Sequentially, this percentage was utilized to backward calculate the trace element level in the primary magma.

Step 3: Set up the parameters in the ABS3. DENOMIN: PM; PERID: Eiler's dataset; geodynamic model: 08_Costa Rica and T-factor: 1.1 ("08_Costa Rica" is the closest to and the most similar arc background to Bocas del Toro; T-factor means the rule temperature plays in the melting process).

Step 4: Try different values of the input parameters to find the best match between the input sample and the simulated outcomes.

Thus, the following diagrams and melting condition for all the representative samples were obtained. From the modeling, it concluded that the preferred Arc basalt simulator results are: A mantle wedge partial melting fraction is of 2.5-6.0%, formed in very dry conditions, with a hydrogenous component of only around 0.1%. The melting pressure ranges from 1.8 to 1.9 Gpa (60km in depth), and the melting temperature 1150-1350°C, and the slab temperature is 964°C with the slab pressure about 5Gpa (165km in depth). The liquid contribution from the sediments is about 20%-40% (A. Table 5).

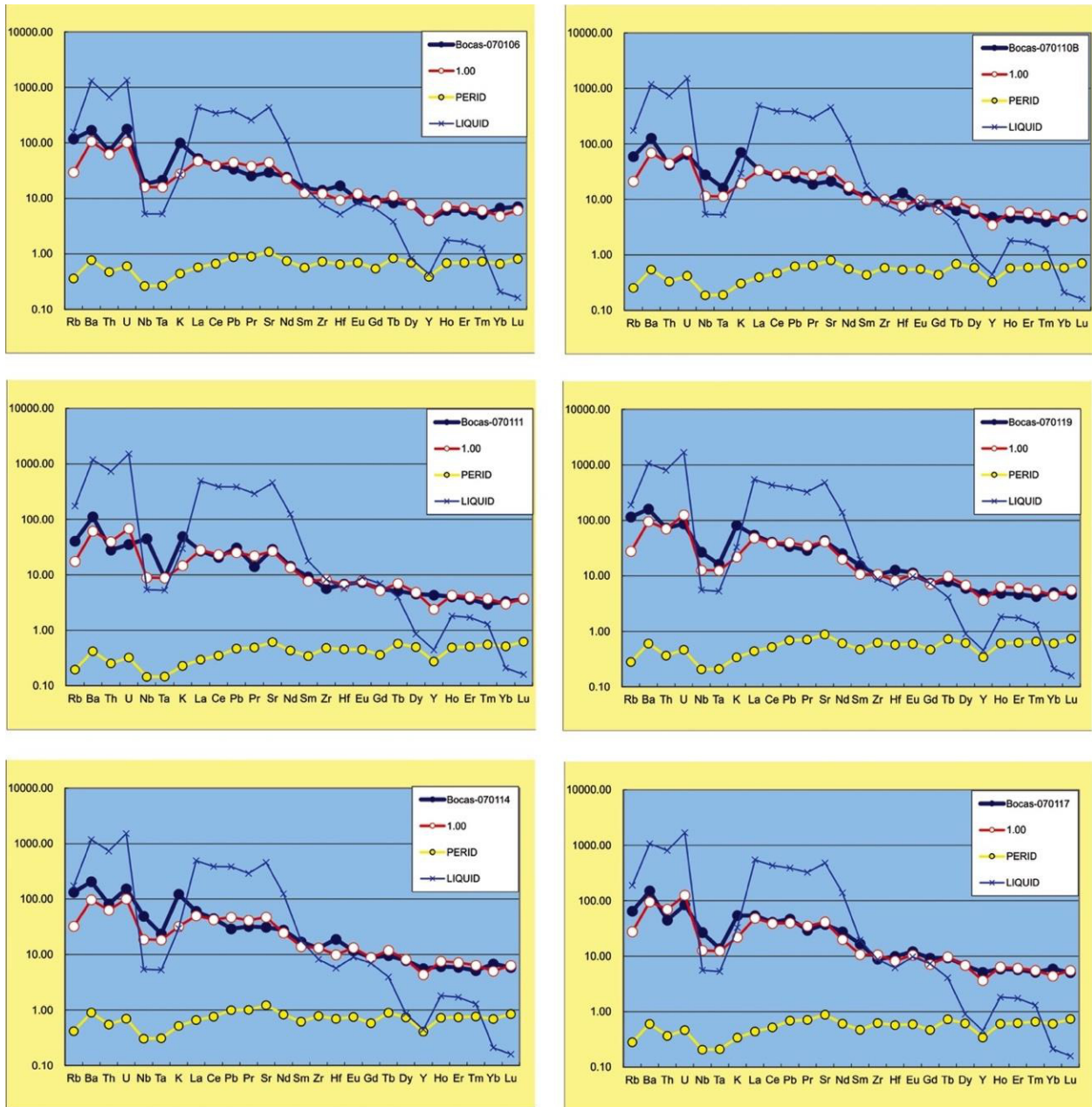


Figure 5.5 Best fit model solutions shown compared to exemplar basalts.

CHAPTER 6

DISCUSSIONS

6.1 Previous Geochemical Models and Evaluation

As for the geochemical variations along the Panamanian arc bridge, Wegner et al. (2010) conducted systematic studies on geochemistry and geochronology of arc igneous rocks in the Panama block. They determined the magmatic evolution and oceanic plate interactions over the past 100 Ma in western Panama, and divided the igneous rocks in the Panamanian arc Isthmus into six groups based on the ages and geochemical differences (Fig. 6.1): 1) Formation of the oceanic basement of the Caribbean large igneous province from 139 to 69 Ma; 2) Younger terranes with enriched geochemical composition were amalgamated at 70 Ma; 3) The geochemical trace element patterns hosted in the Azuero and Soná peninsulas (Soná-Azuero arc) suggested the initiation of subduction at 71–69 Ma; 4) Arc magmatic activities continued in the Chagres region (Chagres-Bayano arc) from 68 to 40 Ma; 5) Discrete volcanoes across the Cordillera de Panama (Cordilleran arc) formed from 19 to 5 Ma; 6) The youngest phase consists of adakitic composition (Adakite suite) in the Cordillera de Panama that developed over the past 2 million years. Wegner's work provides an evolutionary framework for the arc rocks in Panama, and of the chemical variations of arc rocks along the history of the arc volcanic evolution in Panama. His work also provides us an ideal database for researching the entire magmatic history in the Central American Land Bridge. In this thesis, the studies concentrated on the geochemical variations and origin of the Miocene Western Panama arc magmatism in western Panama.

Abratis et al. (2001) identified that small volumes of adakitic and alkalic backarc lavas erupted between 5.8 and 2 Ma and have geochemical and isotopic compositions indicating derivation from the Galapagos plume. Abratis et al. explained it as the products of the an influx of Pacific upper mantle into the Caribbean mantle wedge through a slab window, where the alkaline rocks formed by melting of the upwelling mantle, and the adakites result from melting of the leading edge of the subducted Cocos Ridge (Fig. 6.2). In this model, Abratis et al. described the source of the enriched OIB-like component and the motion rate of the upper mantle flow beneath Central America from southern Costa Rica northward. However, one problem with the model is that the spreading ridge at the time (during the Sandra rift) is still preserved off shore south of

Panama. More evidence is still needed to support the hypothesis and the timing of the influx of enriched chemical source from the Galapagos plume and its tracks.

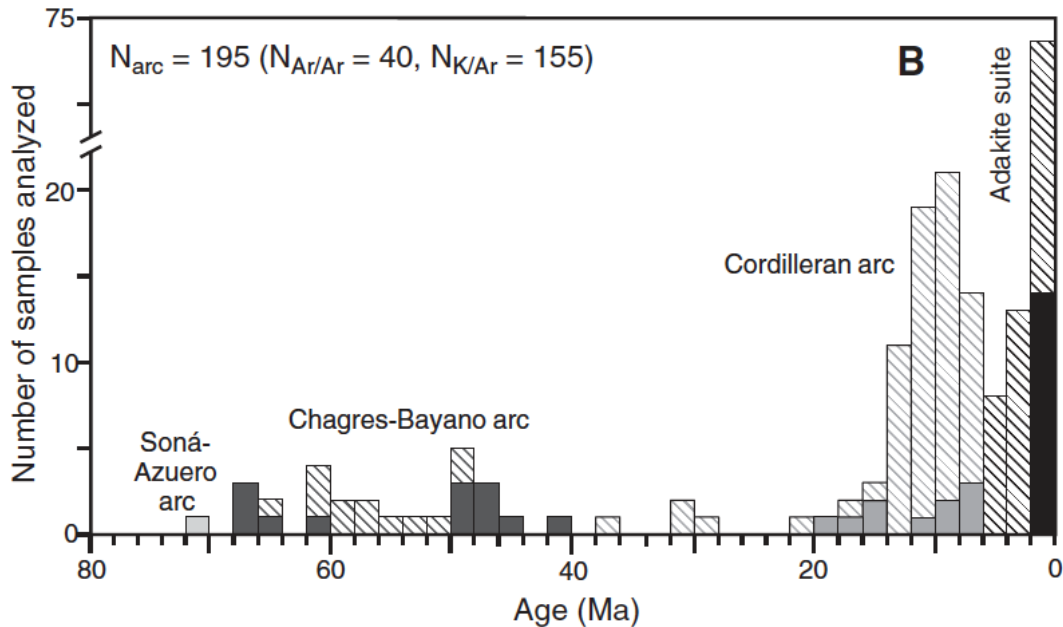


Figure 6.1 Age distribution of arc rocks in central and western Panama and in southern Costa Rica (Wegner et al., 2010). Gray bars- $^{40}Ar/^{39}Ar$ data from (Abratis 2001, Worner 2009); hatched bars-K/Ar data from Kesler et al. (1977); de Boer et al. (1991); Drummond et al. (1995).

Herrstrom et al. (1995) noted that lavas from northern and central Costa Rica have geochemical compositions indicating an enriched mantle source that has been influenced by the subducting slab. They suggested that asthenospheric mantle is flowing northward behind the subducting Nazca plate around the northwest corner of South America. Lavas from central Nicaragua have trace element and isotopic composition indicating that they are derived from relatively depleted mantle with a long history of interaction with the subducting Cocos plate. Gazel et al. (2009) cast doubt on the hypothesis about the origin of the enriched composition based upon the lack of a high $^{208}Pb/^{204}Pb$ isotopic composition for the volcanic rocks in eastern Panama. This signature should be observed for northward flow beneath the Nazca Plate based on the hypothesis of asthenosphere flow.

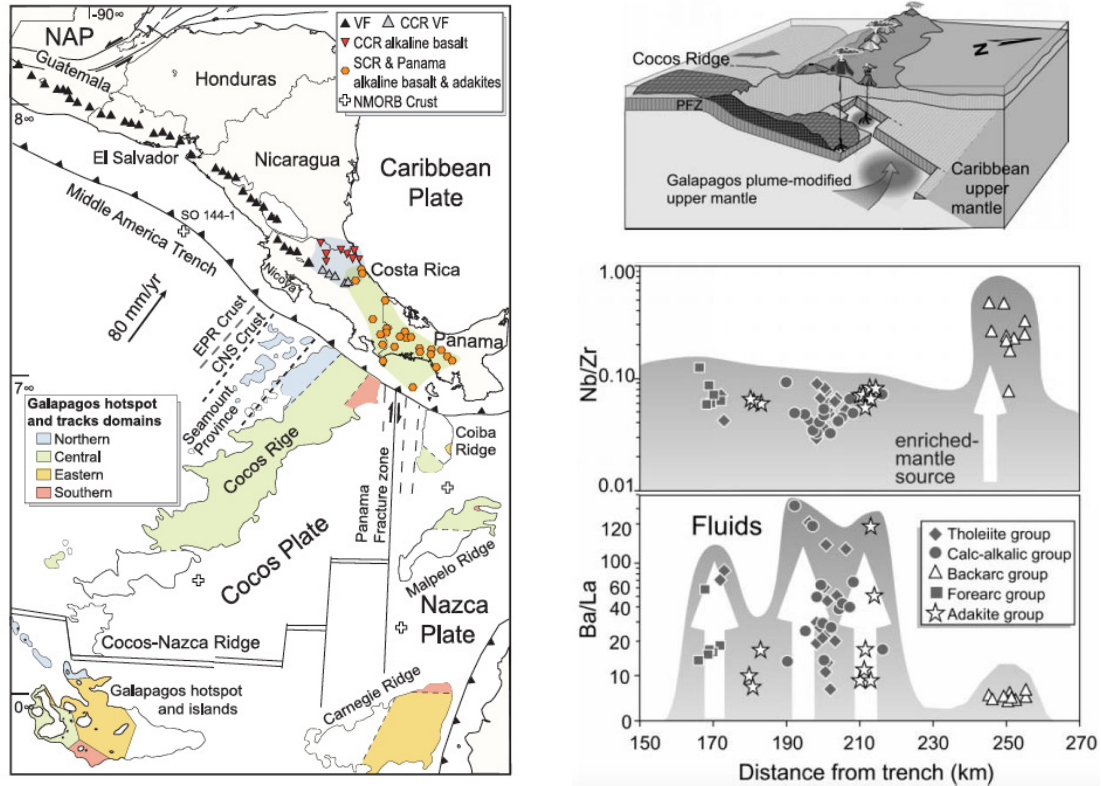


Figure 6.2 Abratis et al.’ schematic model of subduction zone beneath Costa Rica showing disruption of Cocos plate as result of the collision and subduction of extinct spreading ridge (Cocos Ridge). Flux of Galapagos plume-modified asthenosphere into mantle wedge of southern Costa Rica occurs through this slab window, while the edge of Cocos Ridge melts to form adakite magmas (Abratis et al., 2001).

Eiler et al. (2000, 2005) quantified the chemical contributions of mantle wedge, slab interior (altered oceanic crust) and top sediments of the plate by constraints on the values of oxygen-isotope ratios of olivine and plagioclase phenocrysts in basalts and basaltic andesites from the Central American arc. Eiler’s research provides more compositional constraints on modeling the partial melting in the mantle wedge, especially in quantifying the contribution from the three end-members forming the melts beneath the arc area. In this thesis, his dataset was also used to model and evaluate the chemical processes in Bocas del Toro arc zone.

Gazel et al. (2009, 2011) proposed that the adakites and alkaline basalt in southern Central America (central Costa Rica and Panama) have isotopic and trace element compositions with an OIB affinity, similar to the Galapagos hotspot lavas. As their hypothesis suggested, the higher Pb isotopic ratios, relatively lower Sr and Nd isotopic ratios, and enriched incompatible element

signature of central Costa Rican magmas can be explained by arc-hot spot interaction, which started to collide with the Panama arc margin 8 Ma ago. Based on their models, the Galapagos hot spot contribution decreases systematically along the volcanic front from central Costa Rica to NW Nicaragua. This theory quantified the contribution of the OIB-like sources and modeled the partial melting in the mantle wedge for arc rocks distributed in the volcanic fronts of Nicaraguan and Costa Rica. But the hypothesis only talks geochemical variations of magmas in Costa Rica, and does not mention the arc-hot spot interaction in the Western Panama, and has not related the geochemical variations to fractional crystallization in the crust, which has a important impact on the formation of magmas and chemical composition.

Farris et al. (2011) interprets the geochemical change around 24 Ma ago as due to the fracturing of the Panama block during initial collision with South America, which simultaneously caused the localized crustal extension, normal faulting system, sedimentary basin, and extensional magmatism in the Canal Basin and Bocas del Toro (Fig. 6.3). Farris et al. suggested that, within the Panama Canal Zone, volcanic activities transitioned from hydrous mantle-wedge-derived arc magmatism to localized extensional arc magmatism at ~24 Ma, and meantime, an enriched mantle source mixed into the subarc environment, and caused the geochemical variations in the Canal Basin and Bocas del Toro Basin areas. However, it should be noted that the Bocas del Toro rocks are significantly younger (12-8 Ma) than those in along the Panama Canal.

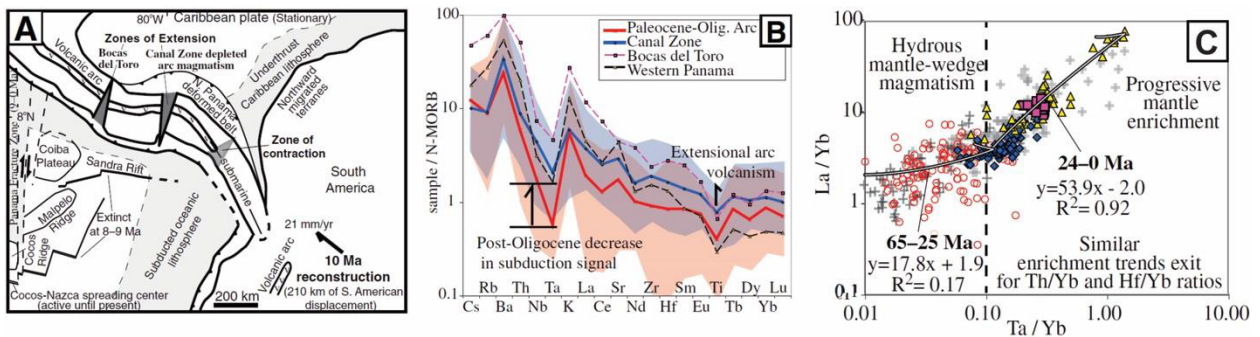


Figure 6.3 Farris et al.’ model regarding the Panamanian tectonic evolution and its effect on the geochemical element changes. A. Tectonic reconstruction at 10 Ma. This is an intermediate step in the collision between South America and Panama. The Panama block has fractured, resulting in two zones of extension (Canal Zone and Bocas del Toro) (Farris et al., 2011).

All of the models provide potential ideas to explain the modeling results from the Bocas del Toro arc, from initial mantle wedge partial melting to fractional crystallization in the crust. A new model was constructed based on previous research and our new geochemical data, and evaluated these models based on how well they fit observational data.

6.2 Arc-hotspot Interaction and Magma Origin

Geologic and geochemical evidence indicates that the back-arc alkaline magmas and young adakites (<2 Ma) in western Panama and eastern Costa Rica represent clear similar geochemical affinity (La/Yb and Th/Yb vs. Ta/Yb) to the Cocos Ridge, Cocos Seamount and therefore the Galapagos hot spot.

The model of partial melting in the mantle wedge indicates that the contribution from the enriched geochemical end-member (80% Cocos Ridge + 20% Seamount Province) and the upper oceanic sediments are ~1.5% and ~0.5%, respectively. The partial fraction (F) of the melting base on the trace element model #1 is around 5%, and this value from the Arc Basalt Simulator version 3 (ABS3) (Kimura et al., 2010) model ranges from 2.5% to 6.0% with a very low hydrous contribution. The three trace elemental models yield consistent results about the melt composition and the melting condition. The models indicate open system melting at a depth of around 60 km (1.8-1.9 GPa) with a temperature of ~1200 ° C, and a slab pressure and temperature during the dehydration of around 5 GPa (165km in depth) and ~964 ° C. The estimated slab melt from AOC and sediment are 5% and 25%, respectively. These models show that the melts formed at a relative deep depth, which is consistent with the backarc location of the Bocas del Toro magmatism. The petrology and geochemistry presented here also suggest that the back-arc alkaline basalts in Bocas del Toro are primarily derived through decompression melting and the interaction of these melts with the subduction-metasomatized lithosphere. The addition of enriched geochemical component into the mantle wedge melts changed the trace element and isotope pattern as examined in the simultaneous arc magmatism and some arc areas in Costa Rica.

6.3 Low-Pressure Fractional Crystallization and Extensional Tectonics

The crustal low-pressure (0.5~1.0 kbars) process of fractional crystallization as modeled in the major element simulations can occur in different geologic settings, for example, Mid-oceanic ridge, extensional magmatism, in a shallow crust environment. Based on the trace element patterns

of igneous rocks from Bocas del Toro and other four groups (Fig. 4.5A and 4.6), their pronounced low Nb-Ta anomaly, and enriched fluid-mobile LILEs, it is easy to rule out the possibility of a mid-oceanic ridge tectonic settings. Even though some samples fall into the MORB area in discrimination diagrams, it is difficult to explain the enrichment of fluid-mobile LILEs observable in its trace element pattern. In addition, the Bocas del Toro lavas are interbedded with marine sedimentary rocks, and therefore support that the basin and the volcanic lavas formed simultaneously. It is rare to form the rock type and interbedded basaltic andesite on the abyssal mid oceanic ridge system. We can deduce that the low pressure occurring during the fractional crystallization was possibly caused by the extensional tectonic change in the western Panama in the Miocene period. The major element modeling in this thesis is consistent with Farris et al. (2011)'s hypothesis regarding the formation of the arc volcanic lavas crystallized during the decompression melting of the subarc asthenosphere, which should be caused by the localized crustal extension, and sequentially formed the sedimentary basin. Farris et al. (2011) conducted detailed investigation in the Canal Basin area, and mapped the stratigraphy and volcanoes in Canal Basin. He found that similar geologic events happened in the canal area by examine the geochemical variations of the rocks from the canal basin lavas. He found the magmas began to crystallize at a relative low pressure, about 1.0 kbars, and the ratios of Ba/Yb, La/Yb and Th/Yb began to decrease due to tectonic change. As the enriched Cocos tracks can't be subducted into the mantle wedge in the Canal Basin area due to the long distance from the Cocos ridge. Farris proposed that there is a relationship between the decrease of fluid mobile elements and decreased crystallization pressure. In addition, basin and normal fault system are developed in this area during the Miocene period, which lead us to hypothesis that the low-pressure process during the crystallization was also caused by the extensional tectonic change. In Bocas del Toro area, it is believed that the low-pressure crystallization was also caused by the crustal extension in the similar tectonic background. These geologic, geochemical and extensional basin formations are also consistent with ongoing collisional process of the Panamanian Block with South America, and the subduction of Cocos Ridge and Cocos Seamount Province.

CHAPTER 7

CONCLUSIONS

To unveil the causes leading to the observed geochemical signature and variations of the Bocas del Toro's arc rocks and the possible effect from the extensional tectonic activities during Miocene period, the geology, geochemistry, mineralogy, tectonics, etc. in western Panama were studied. Additionally, the key data from all the similar rocks from the western Panamanian Isthmus were collected and compared with those of the Bocas del Toro area. Consequently, the following conclusions concerning the geochemical variation, the partial melting and fractional crystallization conditions of the Bocas del Toro arc volcanic rocks were reached.

The volcanic rocks of Bocas del Toro consist of trachy-basalt to trachy-andesite with SiO₂ ranging from 45 wt. % to 64 wt. %, and show a high content of potassium and low content of magnesium. These rocks are amongst the most alkaline in all of Panama. The Bocas del Toro rocks also exhibit a slightly decreased slab dehydration signature with a low Nb-Ta anomaly, enriched fluid-mobile LILEs and low Ti content. Miocene and younger Panama/Costa Rica volcanic rocks were divided into five groups: main arc tholeiite (~17-11 Ma) and calc-alkaline (~12-8 Ma), backarc alkaline (~8-2 Ma) and Bocas del Toro (~12-8 Ma), and adakite (< 2 Ma) groups.

In terms of trace element ratios and isotope geochemistry, the Bocas del Toro rocks have low Ba/La, and have values that are higher, but approach the Cocos Ridge/Galapagos hot spot. The La/Yb and Th/Yb vs. Ta/Yb also show values that plot between the tholeiite and general calc-alkaline groups. Constraints from the referenced Pb-Nd-Sr isotopes suggest that about 1-3% of the enriched composition from the Cocos tracks contributed into the mantle wedge melts during the period of calc-alkaline and backarc alkaline formation.

The MELTS software was used for major element modeling and shows us that the Bocas rocks underwent low-pressure (~1 kbars) fractional crystallization, from 1200 ° C to 900° C with 50%-55% fractionation from a starting magma with ~11 wt. % MgO. The low crystallization pressure leads us to the hypothesis that there was an extensional tectonic change during the period, combining the evidences of tectonics and basinal structure.

The processes of partial melting in the mantle wedge were modeled employing the inverse trace element models and the ARC BASALT SIMULATOR 3.0. These models indicate a component of enriched OIB-like end-member influx into the mantle wedge melts. We also show

that the mantle wedge underwent 2.5%-6.0% of melting under dry conditions at pressures of 1.8 Gpa to 1.9 Gpa (~60km) with temperatures of 1150-1350°C. The slab pressure and temperature beneath the zone of mantle wedge melting is around 5 GPa (165km in depth) and ~964 ° C, respectively, and the estimated slab melt from AOC (altered oceanic crust) and sediments are 5% and 25%, respectively. The deep slab depth is consistent with the current back arc location of Bocas del Toro.

In conclusion, we suggest that the geochemical variations of Bocas del Toro were caused by an influx of an OIB-like component into the mantle wedge by 12 Ma, and that crustal extension reduced the overall subduction signature.

APPENDIX A

TABLES

Table A. 1 Major and trace element compositions of Bocas del Toro

Sample ID	70106	70107	70108	70109	70110	70111	70112	70113	70114	70116	70117	70118	70119
SiO ₂	51.18	56.23	59.18	63.89	63.15	48.87	51.42	55.48	59.44	52.02	44.78	51.77	52.20
TiO ₂	0.85	1.10	1.11	0.61	0.92	1.03	1.04	1.01	0.78	1.19	1.22	1.40	1.10
Al ₂ O ₃	15.81	17.12	16.48	14.90	15.52	19.00	17.58	16.82	17.71	18.87	17.17	17.48	19.84
FeO _t	4.89	6.27	6.74	3.74	3.46	7.05	7.45	7.20	3.02	7.27	8.15	6.37	6.28
MnO	0.23	0.17	0.16	0.07	0.10	0.16	0.13	0.16	0.08	0.21	0.24	0.24	0.14
MgO	1.35	1.21	1.39	0.50	0.81	3.43	3.34	1.73	0.35	2.45	3.31	1.76	2.03
CaO	8.03	5.86	4.14	2.79	4.88	5.88	5.42	5.90	3.98	6.17	9.98	7.59	6.89
Na ₂ O	3.63	3.42	3.49	3.72	3.51	4.38	4.76	3.44	4.02	3.62	3.9	3.77	4.05
K ₂ O	4.15	3.94	4.73	3.04	2.92	2.04	3.73	3.87	5.12	4.47	2.26	4.45	3.41
P ₂ O ₅	0.08	0.29	0.03	0.00	0.00	0.07	0.12	0.00	0.01	0.29	0.18	0.74	0.12
Sum	90.20	95.61	97.46	93.27	95.27	91.91	94.99	95.62	94.50	96.58	90.97	95.57	96.07
Sc	9.72	17.06	14.62	10.91	14.94	23.45	24.39	16.77	8.23	11.59	14.50	19.59	12.03
V	68.04	155.82	81.97	47.70	117.76	228.34	220.78	124.18	58.51	185.40	188.53	208.55	179.55
Cr	1.56	3.92	1.76	10.04	3.36	5.43	2.17	4.27	2.38	2.71	2.84	2.47	1.89
Co	7.67	18.42	12.32	11.83	10.57	18.25	17.14	18.75	6.50	15.12	18.83	13.14	14.72
Ni	31.00	38.00	38.00	38.00	38.00	45.00	46.00	51.00	35.00	46.00	51.00	51.00	45.00
Zn	91.48	99.29	99.80	50.32	71.53	84.78	63.71	106.12	76.14	105.03	103.50	138.77	97.70
Rb	103.41	103.04	127.16	61.78	52.22	35.64	50.30	107.87	117.35	110.56	57.20	102.39	101.85
Sr	623.78	536.29	369.28	430.65	450.39	612.84	444.31	537.07	659.07	902.08	795.70	805.72	918.52
Zr	208.42	175.21	235.37	142.76	140.64	84.00	91.97	148.38	194.94	171.71	132.61	192.68	154.47
Nb	18.87	19.04	23.63	16.32	14.28	7.82	10.37	18.53	20.91	16.66	12.07	17.85	14.45
Cs	1.76	1.80	2.44	0.87	0.56	0.47	0.21	1.85	2.20	0.99	0.76	0.58	0.75
Ba	1278.37	1155.14	1369.41	1200.36	955.88	842.31	983.57	1096.65	1555.93	1391.91	1133.46	1332.20	1209.94
La	41.32	42.07	46.37	32.83	26.83	21.39	27.38	40.48	47.32	50.72	42.56	57.96	42.89
Ce	77.51	82.94	90.84	60.32	53.59	41.97	54.49	80.07	90.47	99.33	83.14	112.42	82.41
Nd	37.40	41.41	43.90	24.96	22.69	22.15	28.55	37.25	42.91	49.27	42.32	51.81	38.92
Sm	8.07	8.68	9.24	5.68	5.95	4.81	5.98	8.22	8.95	10.03	8.77	11.87	8.08
Eu	1.88	2.06	1.92	1.36	1.54	1.43	1.70	2.00	2.28	2.49	2.38	2.90	2.23
Tb	1.09	1.22	1.27	0.86	0.83	0.67	0.77	1.23	1.26	1.34	1.23	1.51	1.03

Table A. 1 - continued

Sample ID	70106	70107	70108	70109	70110	70111	70112	70113	70114	70116	70117	70118	70119
Dy	7.24	7.49	7.85	4.75	5.18	4.18	4.84	7.28	7.24	6.29	6.36	7.58	5.51
Yb	3.96	4.00	4.65	3.17	2.82	1.97	2.31	3.74	4.05	3.76	3.52	4.75	2.97
Lu	0.63	0.63	0.68	0.54	0.44	0.33	0.37	0.51	0.52	0.49	0.45	0.61	0.41
Hf	6.90	7.13	8.77	6.17	5.40	2.78	3.88	7.02	7.74	6.24	4.08	6.72	5.24
Ta	1.11	1.12	1.39	0.96	0.84	0.46	0.61	1.09	1.23	0.98	0.71	1.05	0.85
Th	8.15	8.54	10.46	6.21	4.75	3.20	4.23	8.34	9.32	9.02	5.11	9.30	8.29
U	5.28	3.58	3.81	2.27	1.94	1.05	1.44	3.02	4.57	4.01	2.53	3.46	2.60

Table A. 2 Mineral-melt distribution coefficients and bulk distribution coefficient

Partition Coefficient	Mineral	Rb	Ba	Th	U	Nb	Ta	K	La	Ce	Sr	Nd	Zr	Sm	Eu	Ti	Dy	Yb	Lu
Villemant 1988; Dunn and Senn, 1994	Ol	0.00 1	0.01	0.02	0.01	0.00 65	0.06 5	0.00 7	0.00 67	0.00 6	0.01	0.00 59	0.01	0.00 7	0.00 74	0.01 3	0.01 3	0.04 91	0.04 54
Adam & Green 2006	Opx	0.00 38	0.00 36	0.00 05	0.00 07	0.00 07	0.00 08	0.00 3	0.00 06	0.00 17	0.00 19	0.00 4	0.00 99	0.01 1	0.03	0.1	0.07 7	0.07 7	0.09
Villemant 1988; Luhr & Carmichael (1980); Forsythe et al. 1994	Cpx	0.03	0.02	0.16	0.02	0.27	0.26 1	0.01	0.05 6	0.09 2	0.00 74	0.23	0.78 6	0.04 45	0.47 4	0.25	0.58 2	1.4	0.50 6
Hauri et al. 1994	Gar	0.00 07	0.00 07	0.00 137	0.00 588	0.05 38	0.05	0.05	0.01 64	0.06 5	0.00 99	0.36 3	2.12	1.1	2.02	0.68 8	4.13	3.88	3.79
Elkins et al. 2008	Spi	0.02 9	0.00 06	0.01	0.01 4	0.00 06	0.00 04		0.00 02	0.01	0.00 47	0.24	0.00 81	0.18	0.01	0.04 8	0.01	0.01	0.00 07

Mineral	Fraction	Rb	Ba	Th	U	Nb	Ta	K	La	Ce	Sr	Nd	Zr	Sm	Eu	Ti	Dy	Yb	Lu
Ol	0.6	0.00 06	0.00 6	0.012	0.006	0.003 9	0.03 9	0.00 42	0.004 02	0.003 6	0.006	0.00 354	0.006	0.004 2	0.004 44	0.00 78	0.00 78	0.02 946	0.02 724
Opx	0.25	0.00 095	0.00 09	0.000 125	0.000 175	0.000 175	0.00 02	0.00 075	0.000 15	0.000 425	0.000 475	0.00 1	0.002 475	0.002 75	0.007 5	0.02 5	0.01 925	0.01 925	0.02 25
Cpx	0.14	0.00 42	0.00 28	0.022 4	0.002 8	0.037 8	0.03 654	0.00 14	0.007 84	0.012 88	0.001 036	0.03 22	0.110 04	0.006 23	0.066 36	0.03 5	0.08 148	0.19 6	0.07 084
Gar	0.01	0.00 0007	0.00 0007	0.000 0137	0.000 0588	0.000 538	0.00 05	0.00 05	0.000 164	0.000 65	0.000 099	0.00 363	0.021 2	0.011	0.020 2	0.00 688	0.04 13	0.03 88	0.03 79
Bulk Distribution Coefficient		0.00 5757	0.00 9707	0.034 5387	0.009 0338	0.042 413	0.07 624	0.00 685	0.012 174	0.017 555	0.007 61	0.04 037	0.139 715	0.024 18	0.098 5	0.07 468	0.14 983	0.28 351	0.15 848

Table A. 3 Modeled #1, #3 Components and melts for the southern Central American lavas (Gazel et al., 2009)

	Rb	Ba	Th	U	Nb	Ta	K	La	Ce	Sr	Nd	Zr	Sm	Eu	Ti	Dy	Yb	Lu
DM (SO 144-1) 8%F (60ol25opx12cpx3spn)	0.0	0.49	0.00	0.00	0.11	0.00	49.8	0.19	0.64	8.49	0.71	6.73	0.3	0.11	1075	0.59	0.39	0.06
“OIB-Like” Mantle Wedge 5%F (52ol29opx16cpx4spn)	61	1	7	2	4	8	09		5	9	8	3		4	.610	6	3	2
															6			
	1.4	33.9	0.29	0.09	1.09	0.06	664.	1.89	4.23	58.6	2.29	13.4	0.49	0.2	1069	0.75	0.43	0.08
	466	3	0				12			1		4			.74			
	6																	
Mean Semount Province melt (SP) 20%F (83cpx15ga2rut)	174	2094	21.0	8.43	62.2	3.26	7139	190.	353.	2755	108.	265.	8.20	1.95	4474	2.51	0.72	0.08
	.7	.676	47	8	17	8	2.9	473	951	.231	962	09	9	1	.777		3	8
															8			
Mean Cocos/Coiba Ridge melt (CCR) 20%F (83cpx15ga2ru)	51.	435.	6.19	4.44	17.1	0.88	1369	63.3	120.	974.	46.8	122.	4.44	1.14	2899	2.20	0.84	0.11
	4	095	9	4	68	3	7.47	42	672	121	03	595	5	6	.988	3	4	
							5								8			
Galapagos Component 2 (SP20% + CCR80%)	76.	767.	9.16	5.24	26.1	1.36	2523	88.7	167.	1330	59.2	151.	5.19	1.30	3214	2.26	0.82	0.10
	06	011	9	3	78		6.56	68	328	.343	34	094	7	7	.946	5		5
															6			
Sediment Melt1 (30Carb + 70Hemi) 20%F (D15garnet84.6cpx0.4rut)	149	1701	10.7	17.3	12.0	0.77	5570	75.4	91.4	3329	38.9	74.3	3.03	1.08	986.	1.40	0.57	0.08
	.15	3.20	38	13	73	1	3.06	45	11	.281	2	87	1	7	4716	2	6	
		3					5											
SedMelt 2(Oligocene-Miocene) (30Carb + 70Hemi) 20%F (D15garnet84.6cpx0.4rut)	149	5671	10.7	3.85	12.0	0.77	5570	75.4	91.4	3329	38.9	74.3	3.03	1.08	986.	1.40	0.57	0.08
	.15	.06	38		73	1	3.06	45	11	.281	2	87	1	7	4716	2	6	
							5											

Table A. 4 Compositions of Model #2, #3 components (Eiler et al, 2004)

	MORB-Like Mantle	OIB-Like Mantle	Low- $\delta^{18}\text{O}$ Slab	High- $\delta^{18}\text{O}$ Slab
	Wedge	Wedge	Phase	Phase
Ba, ppm	0.317	33.93	2573	614
U, ppm	0.0042	0.09	2.6	0.28
Th, ppm	0.011	0.25	2.75	1.25
K ₂ O, wt. %	0.03	0.08	2.1	0.3
Nb, ppm	0.137	1.09	14.7	0.5
La, ppm	0.138	1.89	25.8	9.3
Pb, ppm	0.031	0.22	17.3	7.9
Ce, ppm	0.44	4.23	59.4	17.5
H ₂ O, wt. %	0.026	0.25	50	10
Nd, ppm	0.472	2.29	40.5	11.5
Sr, ppm	5.87	58.61	3071	921
Zr, ppm	5.45	13.44	215	25
Sm, ppm	0.2	0.49	9.7	1.6
Cu, ppm	4.8	5.67	1150	32
Na ₂ O, wt. %	0.2	0.24	8	2.1
TiO ₂ , wt. %	0.17	0.18	0.75	0.1
Yb, ppm	0.48	0.43	0.5	0.5
$\delta^{18}\text{O}$ olivine	5	5.1	0	25

Table A. 5 Outcome of modeling of basalts in the Bocas del Toro Basin (Eiler et al., 2005)

Sample	Slab Liquid Fraction			Slab P	Slab	%MORB ext.	MELTING	MELTING	Fslb
	Fliq(AOC)	Fliq(SED)	Fliq(DM)	(GPa)	T(C)		P(GPa)	T(C)	liq.%
Bocas-070111	0.7	0.3	0	5	964	6	1.9	1200	0.05
Bocas-070112	0.8	0.2	0	5	964	5	1.9	1200	0.1
Bocas-070106	0.6	0.4	0	5	964	3	1.8	1200	0.08
Bocas-070110	0.7	0.3	0	5	964	4.5	1.8	1200	0.05
Bocas-070114	0.7	0.3	0	5	964	2.5	1.8	1200	0.06
Bocas-070117	0.8	0.2	0	5	964	4	1.8	1200	0.1
Bocas-070119	0.8	0.2	0	5	964	4	1.8	1200	0.1

REFERENCES

- Abratis, M., & Wörner, G. (2001). Ridge collision, slab-window formation, and the flux of Pacific asthenosphere into the Caribbean realm. *Geology*, 29(2), 127-130.
- Barat, F., de Lépinay, B. M., Sosson, M., Müller, C., Baumgartner, P. O., & Baumgartner-Mora, C. (2014). Transition from the Farallon Plate subduction to the collision between South and Central America: Geological evolution of the Panama Isthmus. *Tectonophysics*, 622, 145-167.
- Coates, A. G., Jackson, J. B., Collins, L. S., Cronin, T. M., Dowsett, H. J., Bybell, L. M., ... & Obando, J. A. (1992). Closure of the Isthmus of Panama: the near-shore marine record of Costa Rica and western Panama. *Geological Society of America Bulletin*, 104(7), 814-828.
- Coates, A. G., Aubry, M. P., Berggren, W. A., Collins, L. S., & Kunk, M. (2003). Early Neogene history of the Central American arc from Bocas del Toro, western Panama. *Geological Society of America Bulletin*, 115(3), 271-287.
- Coates, A. G., McNeill, D. F., Aubry, M. P., Berggren, W. A., & Collins, L. S. (2005). An introduction to the geology of the Bocas del Toro Archipelago, Panama. *Caribbean Journal of Science*, 41(3), 374-391.
- de Boer, J. Z., Defant, M. J., Stewart, R. H., & Bellon, H. (1991). Evidence for active subduction below western Panama. *Geology*, 19(6), 649-652.
- Eiler, J. M., Crawford, A., Elliott, T., Farley, K. A., Valley, J. W., & Stolper, E. M. (2000). Oxygen isotope geochemistry of oceanic-arc lavas. *Journal of Petrology*, 41(2), 229-256.
- Eiler, J. M., Carr, M. J., Reagan, M., & Stolper, E. (2005). Oxygen isotope constraints on the sources of Central American arc lavas. *Geochemistry, Geophysics, Geosystems*, 6(7).
- Farris, D. W., Jaramillo, C., Bayona, G., Restrepo-Moreno, S. A., Montes, C., Cardona, A., & Valencia, V. (2011). Fracturing of the Panamanian Isthmus during initial collision with South America. *Geology*, 39(11), 1007-1010.
- Feigenson, M. D., Carr, M. J., Maharaj, S. V., Juliano, S., & Bolge, L. L. (2004). Lead isotope composition of Central American volcanoes: Influence of the Galapagos plume. *Geochemistry, Geophysics, Geosystems*, 5(6).
- Gazel Dondi, E. (2009). Interaction of the Galapagos plume with the southern Central American volcanic front (Doctoral dissertation, Rutgers University-Graduate School-New Brunswick).

- Gazel-Dondi, E., Carr, M. J., Hoernle, K., Feigenson, M. D., Szymanski, D., Hauff, F., & van den Bogaard, P. Galapagos-OIB signature in southern Central America: Mantle refertilization by arc-hot spot interaction. *Geochemistry, Geophysics, Geosystems*.
- Gazel, E., Hayes, J. L., Hoernle, K., Kelemen, P., Everson, E., Holbrook, W. S., & Yogodzinski, G. M. (2015). Continental crust generated in oceanic arcs. *Nature Geoscience*, 8(4), 321-327.
- Gazel, E., Hoernle, K., Carr, M. J., Herzberg, C., Saginor, I., Van den Bogaard, P., & Swisher, C. (2011). Plume–subduction interaction in southern Central America: Mantle upwelling and slab melting. *Lithos*, 121(1), 117-134.
- Gualda, G. A., & Ghiorso, M. S. (2015). MELTS_Excel: A Microsoft Excel-based MELTS interface for research and teaching of magma properties and evolution. *Geochemistry, Geophysics, Geosystems*, 16(1), 315-324
- Hastie, A. R., Mitchell, S. F., Kerr, A. C., Minifie, M. J., & Millar, I. L. (2011). Geochemistry of rare high-Nb basalt lavas: Are they derived from a mantle wedge metasomatised by slab melts?. *Geochimica et Cosmochimica Acta*, 75 (17), 5049-5072.
- Herrstrom, E. A., Reagan, M. K., & Morris, J. D. (1995). Variations in lava composition associated with flow of asthenosphere beneath southern Central America. *Geology*, 23(7), 617-620.
- Herzberg, C., & Asimow, P. D. (2008). Petrology of some oceanic island basalts: PRIMELT2. XLS software for primary magma calculation. *Geochemistry, Geophysics, Geosystems*, 9(9).
- Herzberg, C., & Gazel, E. (2009). Petrological evidence for secular cooling in mantle plumes. *Nature*, 458(7238), 619-622.
- Hidalgo, P. J., & Rooney, T. O. (2010). Crystal fractionation processes at Baru volcano from the deep to shallow crust. *Geochemistry, Geophysics, Geosystems*, 11(12).
- Hidalgo, P. J., & Rooney, T. O. (2014). Petrogenesis of a voluminous Quaternary adakitic volcano: the case of Baru volcano. *Contributions to Mineralogy and Petrology*, 168(3), 1-19.
- Hidalgo, P. J., Vogel, T. A., Rooney, T. O., Currier, R. M., & Layer, P. W. (2011). Origin of silicic volcanism in the Panamanian arc: evidence for a two-stage fractionation process at El Valle volcano. *Contributions to Mineralogy and Petrology*, 162(6), 1115-1138.
- Hoernle, K., Werner, R., Morgan, J. P., Garbe-Schönberg, D., Bryce, J., & Mrazek, J. (2000). Existence of complex spatial zonation in the Galápagos plume. *Geology*, 28(5), 435-438.
- Hoernle, K., van den Bogaard, P., Werner, R., Lissinna, B., Hauff, F., Alvarado, G., & Garbe-Schönberg, D. (2002). Missing history (16–71 Ma) of the Galápagos hotspot: Implications for the tectonic and biological evolution of the Americas. *Geology*, 30(9), 795-798.

- Hoernle, K., Hauff, F., & van den Bogaard, P. (2004). 70 my history (139–69 Ma) for the Caribbean large igneous province. *Geology*, 32(8), 697-700.
- Kelemen, P. B., Yogodzinski, G. M., & Scholl, D. W. (2003). Along-strike variation in the Aleutian island arc: Genesis of high Mg# andesite and implications for continental crust. *Inside the Subduction Factory*, *Geophys. Monogr. Ser.*, 138, 223-276.
- Kesler, S. E., Sutter, J. F., Issigonis, M. J., Jones, L. M., & Walker, R. L. (1977). Evolution of porphyry copper mineralization in an oceanic island arc; Panama. *Economic Geology*, 72(6), 1142-1153.
- Kimura, J. I., Kent, A. J., Rowe, M. C., Katakuse, M., Nakano, F., Hacker, B. R., & Stern, R. J. (2010). Origin of cross-chain geochemical variation in Quaternary lavas from the northern Izu arc: using a quantitative mass balance approach to identify mantle sources and mantle wedge processes. *Geochemistry, Geophysics, Geosystems*, 11(10).
- Le Bas, M. J., & Streckeisen, A. L. (1991). The IUGS systematics of igneous rocks. *Journal of the Geological Society*, 148(5), 825-833.
- Dudek, A., Keller, J., Lameyre, J., Le Bas, M. J., Sabine, P. A., Schmid, R., & Zanettin, B. (1989). A classification of igneous rocks and glossary of terms: Recommendations of the International Union of Geological Sciences Subcommittee on the Systematics of Igneous Rocks (Vol. 193). R. W. Le Maitre (Ed.). Oxford: Blackwell.
- Drummond, M. S., Bordelon, M., De Boer, J. Z., Defant, M. J., Bellon, H., & Feigenson, M. D. (1995). Igneous petrogenesis and tectonic setting of plutonic and volcanic rocks of the Cordillera de Talamanca, Costa Rica-Panama, Central American arc. *American Journal of Science*, 295(7), 875.
- McNeill, D. F., Coates, A. G., Budd, A. F., & Borne, P. F. (2000). Integrated paleontologic and paleomagnetic stratigraphy of the upper Neogene deposits around Limon, Costa Rica: A coastal emergence record of the Central American Isthmus. *Geological Society of America Bulletin*, 112(7), 963-981.
- Montes, C., Cardona, A., Jaramillo, C., Pardo, A., Silva, J. C., Valencia, V., & Niño, H. (2015). Middle Miocene closure of the Central American Seaway. *Science*, 348(6231), 226-229.
- Pearce, J. A., Harris, N. B., & Tindle, A. G. (1984). Trace element discrimination diagrams for the tectonic interpretation of granitic rocks. *Journal of petrology*, 25(4), 956-983.
- Patino, L. C., Carr, M. J., & Feigenson, M. D. (2000). Local and regional variations in Central American arc lavas controlled by variations in subducted sediment input. *Contributions to Mineralogy and Petrology*, 138(3), 265-283.

- Rickwood, P. C. (1989). Boundary lines within petrologic diagrams which use oxides of major and minor elements. *Lithos*, 22(4), 247-263.
- Rooney, T. O., & Deering, C. D. (2014). Conditions of melt generation beneath the Taupo Volcanic Zone: The influence of heterogeneous mantle inputs on large-volume silicic systems. *Geology*, 42(1), 3-6.
- Shaw, D. M. (1970). Trace element fractionation during anatexis. *Geochimica et Cosmochimica Acta*, 34(2), 237-243.
- Smith, Ian EM, Tim J. Worthington, Richard C. Price, and John A. Gamble. "Primitive magmas in arc-type volcanic associations: examples from the southwest Pacific." *Canadian Mineralogist* 35 (1997): 257-274.
- Sun, S. S., & McDonough, W. F. (1989). Chemical and isotopic systematics of oceanic basalts: implications for mantle composition and processes. Geological Society, London, Special Publications, 42(1), 313-345.
- Thompson, A. B. (1976). Mineral reactions in pelitic rocks; II, Calculation of some PTX (Fe-Mg) phase relations. *American Journal of Science*, 276(4), 425-454.
- Wegner, W., Wörner, G., Harmon, R. S., Simon, K., & Singer, B. B. (2007, August). Evolution of a maturing arc system: The west-central Isthmus of Panama. In *Goldschmidt Conf. Abstr* (Vol. 71, p. A1097).
- Wegner, W., Wörner, G., Harmon, R. S., & Jicha, B. R. (2011). Magmatic history and evolution of the Central American Land Bridge in Panama since Cretaceous times. *Geological Society of America Bulletin*, 123(3-4), 703-724.
- Werner, R., Hoernle, K., Barckhausen, U., & Hauff, F. (2003). Geodynamic evolution of the Galápagos hot spot system (Central East Pacific) over the past 20 my: Constraints from morphology, geochemistry, and magnetic anomalies. *Geochemistry, Geophysics, Geosystems*, 4(12).
- Wood, D. A. (1980). The application of a Th Hf Ta diagram to problems of tectonomagmatic classification and to establishing the nature of crustal contamination of basaltic lavas of the British Tertiary Volcanic Province. *Earth and planetary science letters*, 50(1), 11-30.
- Workman, R. K., & Hart, S. R. (2005). Major and trace element composition of the depleted MORB mantle (DMM). *Earth and Planetary Science Letters*, 231 (1), 53-72.
- Wörner, G., Harmon, R. S., & Wegner, W. (2009). Geochemical evolution of igneous rocks and changing magma sources during the formation and closure of the Central American land bridge of Panama. *Geological Society of America Memoirs*, 204, 183-196.

BIOGRAPHICAL SKETCH

Full Name: Ruiguang Pan

Date of Birth: Feb. 18, 1987

EDUCATION:

Dec. 2015 M. Sc. in Geochemistry and Tectonics

Florida State University, Tallahassee, FL

July 2013 M. Sc. in Economic Geology

China University of Geosciences, Beijing, China

July 2010 B. Sc. in Geology

Northeastern University, Shenyang, China

PUBLICATIONS

Zhao, R., Liu, X., Pan, R., Zhou, M., 2015, Element behaviors during alteration and mineralization: A case study of the Xinli (altered rock type) gold deposit, Jiaodong Peninsula, *Acta Petrologica Sinica*.

Deng, J., Wang Q., Liu, X., Pan, R., Zhao, R., 2014, Origin of the Xinli gold deposit, Jiaodong peninsula, China: constraints from fluid inclusion and C–D–O–S–Sr isotope compositions, *Ore Geology Review*.

Yang, L., Wang, Q., Liu, X., Zhang, Y., Pan, R., Feng, Y., 2014, Compositions and Genesis of the Fault Gouge in the Ore-controlling Fault in Jiaodong Peninsula: A Case Study from the Xinli Gold Deposit, *Geotectonica et Metallogenia*.